Atomic Layer Deposition of High Permittivity Oxides: Film Growth and *In Situ* Studies

Antti Rahtu

Laboratory of Inorganic Chemistry
Department of Chemistry
Faculty of Science
University of Helsinki
Finland

———

Academic Dissertation

To be presented with the permission of the Faculty of Science of the University of Helsinki for public criticism in Auditorium A129 of the Department of Chemistry, A. I. Virtasen aukio 1, on September 20th, 2002 at 12 o'clock noon.

HELSINKI 2002

ISBN 952-91-4999-9 (print)
ISBN 952-10-0646-3 (pdf)
http://ethesis.helsinki.fi
Helsinki 2002
Yliopistopaino

Supervisors

Dr. Mikko Ritala
and
Prof. Markku Leskelä
Laboratory of Inorganic Chemistry
Department of Chemistry
University of Helsinki
Finland

Reviewers

Prof. Lauri Niinistö
Laboratory of Inorganic and Analytical Chemistry
Helsinki University of Technology
Finland

Mr. Jaan Aarik
Institute of Physics
University of Tartu
Estonia

Opponent

Prof. Michael L. Hitchman
Department of Pure and Applied Chemistry
University of Strathclyde
U.K.

Science is art,
which copies nature's norms
but not its forms.

Tiede on taidetta,
joka matkii luontoa
vaan ei sen muotoa.

Inspired by: / Mukaellen:
Umberto Eco: "The Name of the Rose "
"Ruusun nimi"

Abstract

In this thesis, several oxide atomic layer deposition (ALD) processes were studied. The main focus was on insulating materials to be used for microelectronic devices. At the moment Al_2O_3, ZrO_2, HfO_2, rare earth oxides and their aluminates and silicates are the most promising materials for metal oxide semiconductor field effect transistors (MOSFETs). In MOSFETs the gate insulator should be deposited in a way that no more than one or two monolayers of SiO_2 would form during the whole device fabrication. $SrTiO_3$ and $Ba_xSr_{1-x}TiO_3$ are the most promising materials for dynamic random access memories (DRAM).

A new method was developed for depositing oxide thin films on silicon by using alkoxides as oxygen sources. Several binary and mixed oxides could be deposited. Of these oxides Al_2O_3 was examined more closely and found to grow on silicon without a SiO_2 interface layer. $Zr_xTi_yO_z$ thin films deposited using this method had a permittivity of 45 - 65 and a leakage current of 10^{-4} A/cm^2 at 0.2 MV/cm.

A detailed understanding of thin film growth mechanism is important. A quadrupole mass spectrometer (QMS) - quartz crystal microbalance (QCM) *in situ* characterization system was developed in this study. QMS monitors the gas phase while QCM the mass changes on the surface. By combining these two methods reaction mechanisms can be examined in real time during the ALD growth in flow-type reactor conditions. The main drawback of QCM is its temperature sensitivity and therefore methods for compensating this effect were developed.

Reaction mechanisms were studied in various oxide processes such as Al_2O_3, TiO_2, ZrO_2, $Zr_xTi_yO_z$, and $SrTiO_3$. Different titanium alkoxides were studied as ALD precursors. The alkoxide group was found to have a strong effect on the ALD reaction mechanism and the stability of the precursor against thermal decomposition. The oxygen source in all binary processes studied was D_2O and thus the main reaction byproduct was the deuterated ligand while in the metal alkoxide - metal halide process two reaction paths were found.

In the $SrTiO_3$ process at 250 ^oC the surface had no effect on the growth rate or reaction mechanism, while at 325 ^oC especially the TiO_2 surface catalyzed the reactions. The change in the growth mechanism was attributed to the formation of crystalline $SrTiO_3$ phase at 325 ^oC instead of a solid mixture of two oxides at 250 ^oC. In addition, *in situ* methods showed a possibility to monitor the metal ratio of ternary films.

Key words: Atomic layer deposition, Oxide, Reaction mechanism, Quadrupole mass spectrometry, Quartz crystal microbalance

List of Publications

The thesis is based on the following original publications and these are referred to in the text by the corresponding Roman numerals:

I M. Ritala, K. Kukli, A. Rahtu, P. I. Räisänen, M. Leskelä, T. Sajavaara, J. Keinonen
Atomic Layer Deposition of Oxide Thin Films with Metal Alkoxides as Oxygen Sources
Science, 288 (**2000**) 319 - 321.

II A. Rahtu, M. Ritala, M. Leskelä
Atomic Layer Deposition of Zirconium Titanium Oxide from Titanium Isopropoxide and Zirconium Chloride
Chem. Mater., 13 (**2001**)1528 - 1532.

III A. Rahtu, M. Ritala
Integration of a Quadrupole Mass Spectrometer and a Quartz Crystal Microbalance for *In Situ* Characterization of Atomic Layer Deposition Processes in Flow Type Reactors
Electrochem. Soc. Proc., 2000-13 (**2000**)105 - 111.

IV A. Rahtu, M. Ritala
Compensation of Temperature Effects in Quartz Crystal Microbalance Measurements
Appl. Phys. Lett., 80 (**2002**) 521 - 523.

V A. Rahtu, T. Alaranta, M. Ritala
In Situ Quartz Crystal Microbalance and Quadrupole Mass Spectrometry Studies of Atomic Layer Deposition of Aluminum Oxide from Trimethylaluminum and Water
Langmuir, 17 (**2001**) 6506 - 6509.

VI A. Rahtu, K. Kukli, M. Ritala
In Situ Mass Spectrometry Study on Atomic Layer Deposition from Metal (Ti, Ta and Nb) Ethoxides and Water
Chem. Mater., 13 (**2001**) 817 - 823.

VII A. Rahtu, M. Ritala
Reaction Mechanism Studies on Titanium Isopropoxide - Water Atomic Layer Deposition Process
Chem. Vap. Deposition., 8 (**2002**) 21 - 28.

VIII A. Rahtu, M. Ritala
Reaction Mechanism Studies on Zirconium Chloride - Water Atomic Layer Deposition Process
J. Mater. Chem., 12 (**2002**) 1484 - 1489.

IX A. Rahtu, M. Ritala
Reaction Mechanism Studies on the Atomic Layer Deposition of $Zr_xTi_yO_z$ Using the Novel Metal Halide - Metal Alkoxide Approach
Manuscript.

X A. Rahtu, T. Hänninen, M. Ritala
In Situ Characterization of Atomic Layer Deposition of $SrTiO_3$
J. Phys. IV, 11(**2001**) Pr3-923 - 930.

Author's contribution

Publication I	The author has done part of the experimental work.
Publications III, IV, VII-IX	The author has done all of the experimental work and written the articles.
Publications II, V, VI, X	The author has done most of the experimental work and written the articles.

List of Acronyms Used

AES	Auger Electron Spectroscopy
ALD	Atomic Layer Deposition
ALE	Atomic Layer Epitaxy
ALCVD	Atomic Layer Chemical Vapor Deposition
CVD	Chemical Vapor Deposition
dc	Direct Current
DRAM	Dynamic Random Access Memory
EBE	Electron Beam Evaporation
EQCM	Electrochemical Quartz Crystal Microbalance
IDR	Incremental Dielectric Reflection
ITO	indium tin oxide (In_2O_3:Sn)
IR	Infrared
LEED	Low Energy Electron Diffraction
LEIS	Low Energy Ion Scattering
MOSFET	Metal Oxide Semiconductor Field Effect Transistor
MS	Mass Spectrometer
PECVD	Plasma Enhanced Chemical Vapor Deposition
PVD	Physical Vapor Deposition
QCM	Quartz Crystal Microbalance
QMS	Quadrupole Mass Spectrometer
RDS	Reflectance Difference Spectroscopy
RHEED	Reflection High Energy Electron Diffraction
SIMS	Secondary Ion Mass Spectroscopy
SPA	Surface Photoabsorption
TFEL	Thin Film Electroluminescent
TPD	Temperature Programmed Desorption
TOF	Time of Flight
TOF-ERDA	Time of Flight Elastic Recoil Detection Analysis
UHV	Ultra High Vacuum
XRD	X-ray Diffraction
XPS	X-ray Photoelectron Spectroscopy

Chemicals

acac	2,4-pentanedione (acetylacetonate)
dmae	$OCH_2CH_2N(CH_3)_2$ (dimethylaminoethoxide)
^{i}Pr	$-CH(CH_3)_2$ (isopropyl)
thd	2,2,6,6-tetramethyl-3,5-heptanedione (tetramethylheptanedione)

Contents

1. Introduction

The tremendous increase in calculation power of computers has changed both the every-day life and research. An exponential growth in performance is rarely met in any field. However, this increase has however not been made without sacrifices. In this case it has been the downscaling of the components on the microelectronic devices. The key component of a modern integrated circuit is a metal oxide field effect transistor (MOSFET). During the past 40 years, actually the whole life of a modern transistor, the downscaling has been made by dividing the physical dimensions of the transistors by a constant. However, at the moment the material properties of the SiO_2 based insulators are approaching the fundamental limits and therefore new materials have to be found. Presently the most promising insulating materials for MOSFETs are Al_2O_3, ZrO_2, rare earth oxides and their aluminates and silicates.[1-5] On the other hand, $SrTiO_3$ and especially $Ba_{1-x}Sr_xTiO_3$ are the most potential materials for dynamic random access memories (DRAM).[6-8]

Insulating thin films can be grown from both liquid and gas phases. The gas phase deposition techniques can be either physical (PVD) or chemical (CVD). The materials used in modern microelectronic applications must have excellent uniformity in both thickness and composition. In addition, very thin and conformal films are needed. Therefore, a very interesting thin film deposition method is atomic layer deposition (ALD). With suitable process parameters all these requirements can be fulfilled with ALD. On the other hand, for new and sophisticated structures a detailed understanding of the process is needed. Therefore, the reaction mechanism studies are important.

Knowledge of the thin film growth mechanisms allows more precise control of the existing processes, and the process parameters for the new processes are easier and faster to find. Usually the *in situ* measurements are fast and large number of process parameters can be studied in a short time. This results in small precursor consumption which is especially important when precursors are expensive or difficult to synthesize.

Flow-type reactors are of greater importance than evacuation-type reactors because their cycle times can be significantly shortened unlike evacuation-type reactors. This is especially important in the production scale because short cycle times allow high throughput. Therefore, the integration of *in situ* equipment to the flow-type reactors is relevant from the industrial point of view. There are only a couple of *in situ* methods which can be used in a normal process environment in a flow-type ALD reactor. These methods can be divided into three groups: optical methods, mass spectrometry and quartz crystal microbalance (QCM). In this work, the integration of QCM and quadrupole mass spectrometer (QMS) to a flow-type ALD reactor is described.**III** The main disadvantage of QCM is the temperature sensitivity and therefore the elimination of this effect is also described.**IV**

The main goal of this thesis was to study new insulating materials to be used as a gate oxide in MOSFET and thus the materials studied (Al_2O_3,**V** TiO_2,**VI, VII** ZrO_2,**VIII** $Zr_xTi_yO_z$**I, II, IX**) have permittivity values in the range of 9 - 40. Usually the problem with high permittivity oxide growth is the easily forming SiO_2 interface layer, which negates the benefits of the high permittivity materials. Therefore, a new method for growing oxide films without strong oxidizer was developed and studied both *ex situ* **I, II** and *in situ*. **IX**

ALD of $SrTiO_3$ was also studied *in situ*.[X] The ternary processes are substantially more difficult to manage than the binary processes and therefore the binary TiO_2 [VI, VII] and SrO processes [X] were studied first.

2. Background

2.1 Metal Oxide Semiconductor Field Effect Transistor

The main focus of this thesis is on materials to be used as gate oxides in MOSFETs. Therefore, the operation of MOSFET will be shortly described. The solid-state transistor was invented at Bell laboratories in 1947. The first MOSFET was fabricated in 1960 by Kahn and Atalla.[9] Since then it has become the main component of modern microprocessors. MOSFET has five main parts: source, drain, channel, gate and gate oxide (Fig. 1).

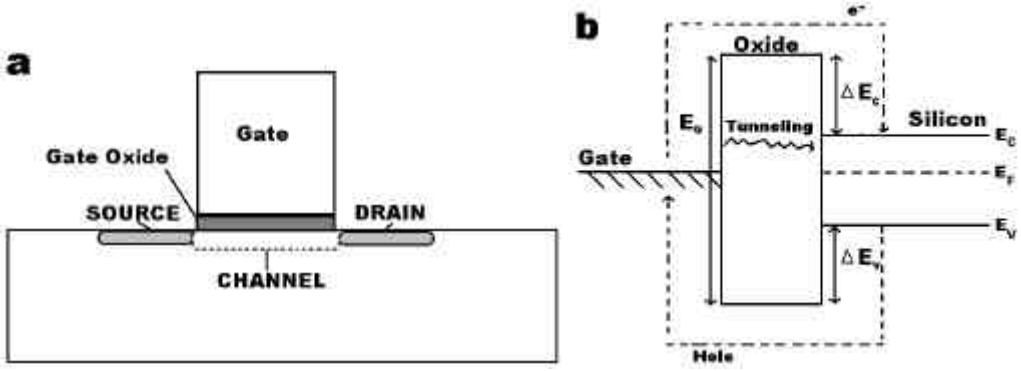

Fig. 1. a) A schematic presentation of a MOSFET transistor and b) the band structure of the gate - gate oxide - channel stack. E_g = band gap, E_f = energy of the Fermi level, E_c= conduction band energy, E_v = valence band energy, DE_c = barrier height between conduction bands in oxide and silicon, DE_v = barrier height between valence bands in oxide and silicon.

The gate voltage controls the current flow from source to drain i.e. the operation of MOSFET. The channel is a different type of semiconductor than the source and drain regions i.e. the current cannot flow through the channel when the transistor is in its off state. When a potential difference is applied to the gate electrode it couples the channel capacitively through the gate oxide and the channel region will be inverted allowing the current to flow from source to drain.

An important property of the gate oxide is the permittivity (e_r) because the gate capacitance (C) is directly proportional to permittivity:

$$C = e_r e_0 A/d \qquad (1)$$

where e_0 is the permittivity of vacuum, A the area and d the thickness of the capacitor.

The leakage current through the oxide should be as small as possible. There are no exact limits for the leakage current but usually upper limits are 1 and 10^{-3} A/cm^2 for desktop and portable applications, respectively.[1] There are two main mechanisms for the leakage current. The first one is the emission of charge carrier i.e. electrons or holes over the dielectric barrier (Fig. 1 b). The band gap (E_g), which is the energy gap between conduction and valence bands, is not always symmetrically aligned with silicon as in

Figure 1 b. Therefore, not only the absolute value of the band gap is important but also its alignment with silicon. The second mechanism for the leakage current is tunneling. Tunneling depends strongly on film thickness and can cause problems with films which are thinner than 1.5 nanometers. With very thin films the tunneling current will be unacceptably high despite the material chosen and thus only the physical film thickness is important.

2.2 Scaling of Microelectronic Devices

Moore's law,[10] which predicts that the number of active elements in the microprocessor doubles every 1.5 - 2 years, has been valid for the last four decades. While the amount of components has increased, their size has decreased. The driving force behind downscaling is faster operating speed and reduction in the production costs. The scaling can be done directly by dividing all physical dimensions by a constant i.e. also the thickness of the gate oxide has to be decreased (see Eq. 1).

The downscaling of a MOSFET sets demands especially on the properties of the gate oxide. SiO_2 based materials have been the choice for the gate oxide for the lifetime of modern transistor. SiO_2 has many good properties such as: high dielectric strength (~ 10^7 V/cm), large band gap (9 eV) and an almost perfect interface with silicon i.e. low interfacial (Si/SiO_2) defect density (~ 10^{10} $eV^{-1}cm^{-2}$, after H_2 passivation).[1] However, the main disadvantage of SiO_2 is its low permittivity (e_r = 3.9). The permittivity of SiO_2 can be increased by mixing it with SiN_y. However, nowadays SiO_xN_y is also approaching the limit where the gate oxide is about to be scaled so thin that the direct tunneling current through it would become unacceptably high. Therefore, new gate oxide materials with higher permittivity are needed. When the permittivity is higher, thicker gate oxides can be used for obtaining a given capacitance and thus the tunneling current is reduced to an acceptable level.

Usually the capacitance of high permittivity materials is compared to SiO_2 i.e. what the theoretical thickness of the oxide layer would be if pure SiO_2 was used. This value is called the equivalent oxide thickness (EOT).

$$\mathrm{EOT} = d\, 3.9/e_r \tag{2}$$

If the gate oxide consists of more than one material, then the capacitance is:

$$\frac{1}{C} = \sum \frac{1}{C_i} \tag{3}$$

where C_i is the capacitance of each capacitor in series.

In terms of EOT:

$$\mathrm{EOT_{total}} = \mathrm{EOT_{High\ permittivity\ layer}} + \mathrm{EOT_{Interface}} \tag{4}$$

To obtain EOT below 1 nm the gate oxide should be deposited in a way that the easily forming interfacial SiO_2 layer would be in maximum two monolayers thick. However, it is a very challenging task due to the strong affinity of silicon towards oxygen.

Interfacial SiO_2 may be formed by two mechanisms: i) a reaction between silicon and a high-permittivity oxide and ii) oxidation of the silicon surface during the oxide deposition.[I] The first mechanism can be avoided by choosing materials that are thermodynamically stable in contact with silicon. From this point of view the most promising and widely studied high permittivity gate oxide materials are Al_2O_3, HfO_2, ZrO_2, rare earth oxides and their aluminates and silicates.[1-5] The second mechanism can be avoided by not exposing the silicon surface to strong oxidizers at the beginning of the high permittivity material growth. This will be discussed in more detail in Chapter 3.4.

In addition to the requirements discussed above the new material also has to have several other properties. The barrier against both hole and electron injection should be at least 1 eV, otherwise the current flow through the insulator might be too high.[2,11] In addition, the band gap alignment with silicon is important. For example Ta_2O_5 has a band gap of 4.4 eV, which would be high enough if it was symmetrically aligned. However, its barrier against electron injection to the conduction band is only 0.3 eV, which is not enough. Figure 2 shows the band gaps and the permittivities of the most widely studied gate oxide materials. It can be seen that the band gap is inversely proportional to the permittivity and therefore for gate oxide applications the preferred permittivity is in the range of 9 - 25.

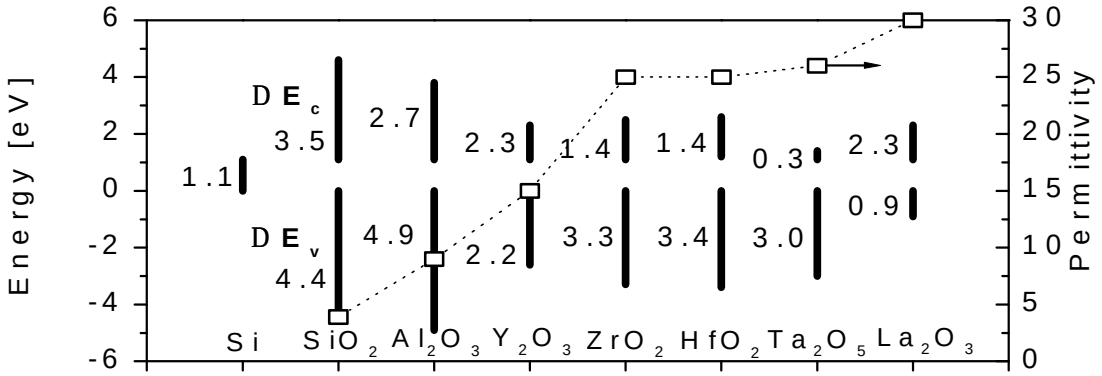

Figure 2. The permittivity, □ $(e_r)^2$ and calculated band gaps of oxides on silicon.[11] DE_c and DE_v are the difference in conduction band and valence band heights between the oxide and silicon (see Fig. 1).

Amorphous gate oxide materials are preferred, because epitaxial oxides are difficult to grow on silicon, and polycrystalline materials usually suffer from leakage current paths along the grain boundaries. Even if the as-deposited material were amorphous it still has to be stable against crystallization during the annealing step for dopant activation where the temperature is usually raised to 900 - 1000 ^oC.[12-14] The crystallization temperature of polycrystalline materials can be increased by mixing them with SiO_2 [4] or, Al_2O_3 [5] i.e. by making silicates or aluminates. For silicates an additional benefit is the better electrical properties of the interface with silicon. The drawback is that the permittivity of the material is decreased as the amount of SiO_2 or Al_2O_3 is increased.[4]

New insulator materials are needed also for DRAMs. The optimal properties of new insulators are slightly different than those for MOSFET and therefore at the moment different materials are studied for these applications. In DRAMs the actual capacitor structure consists of a metal - insulator - metal (MIM) film stack. This allows the use of

oxides, like Ta_2O_5 and TiO_2, which are not stable in direct contact with silicon. In DRAM applications the preferred permittivity is usually higher than in MOSFETs. The band gap requirement is also not as strict because the Schottky barrier i.e. the barrier against electron injection through insulator can be increased with high work function electrodes. Platinum, ruthenium, RuO_2, and $SrRuO_3$ have been proposed for the electrode materials.[6,7] RuO_2 and $SrRuO_3$ have the advantage of being easier to etch than the proposed metals.

The highest storage capacity can be obtained only with three-dimensional memory structures. Therefore, the conformality of the films is a very important issue. PVD methods suffer from rather poor conformality. CVD methods are capable of producing films with good conformality at low temperatures where surface reactions are the rate-limiting step. However, at higher temperatures the rate-limiting step is mass transportation and therefore the conformality starts to deteriorate especially in deep trenches. Therefore, ALD is needed in the future.

2.3 Atomic Layer Deposition

ALD, originally called atomic layer epitaxy (ALE), was developed in Finland in the mid 70s.[15] Several different names such as atomic layer chemical vapor deposition, atomic layer growth, pulsed beam chemical vapor deposition, molecular layer epitaxy, molecular layering, and digital layer epitaxy have been used instead of ALD.[16-18] However, the basic idea is the same despite the different names. For growing amorphous and polycrystalline films, ALD is the most descriptive name and will be used throughout this thesis.

ALD is a gas phase method for depositing high quality thin films.[15,19-22] ALD is based on alternate saturative surface reactions. Each precursor is pulsed into the reaction chamber alternately, one at a time, and the pulses are separated by inert gas purging periods. With properly chosen growth conditions, the reactions are saturative and the film growth is thereby self-limiting. This offers a lot of practical advantages, such as excellent conformality, accurate and simple thickness control and large area uniformity.[16,23-25]

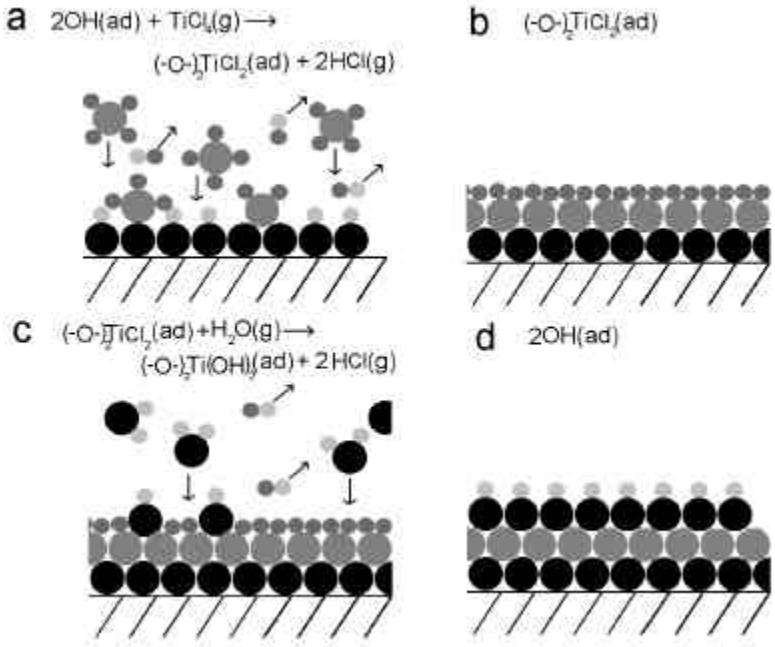

Figure 3. Idealized picture of mechanism for one ALD cycle of TiO_2 growth from $TiCl_4$ and H_2O.

Figure 3 shows a schematic diagram of one ALD cycle of TiO_2 from $TiCl_4$ and H_2O. First $TiCl_4$ is pulsed into the reaction chamber and a layer of precursor is chemisorbed on substrates (Fig. 3 a). After the metal precursor pulse the excess of precursor is purged with an inert carrier gas (Fig. 3 b). Next water is pulsed into the reactor and it reacts with the chemisorbed titanium chloride (Fig. 3 c). The reaction byproducts and excess of water are purged with an inert carrier gas (Fig. 3 d). After the second purge the surface consists of the same functional groups as in the beginning of the ALD cycle and thus it is ready for the next ALD cycle. If each step is saturative, self-limiting growth is achieved and each ALD cycle deposits in maximum one monolayer of the desired material. The density of metal atoms deposited per cycle depends on the temperature, precursor combination and the reactive sites on the surface and therefore only rarely is a full monolayer growth per cycle obtained. The required thickness can be obtained simply by repeating these ALD cycles. The process description was simplified and the possible side reactions affecting the growth are discussed in Chapters 4.5 and 6.

The ALD reactors can be divided into two types: evacuation and flow-type reactors. In evacuation-type reactors the precursor is pulsed into the reactor and after a certain reaction time the reaction chamber is evacuated and is ready for the next precursor pulse. These precursor pulse and pump down cycles are repeated until the desired film thickness is obtained. This is usually time-consuming, and rather expensive pumps such as turbomolecular or diffusion pumps are needed. An additional drawback is the pressure change, which may cause particle formation due to the film peeling off the reaction chamber walls. The evacuation type reactors resemble the pulse modulated MBE reactors. The advantage of these reactors is that it is easy to ensure that the precursor pulses are not overlapping because the pressure of residual gases can be measured directly by a simple pressure gauge. In addition, some reactions appear to take place only in evacuation-type reactors. One example is pyridine catalyzed SiO_2 growth[26-28] from $SiCl_4$ and H_2O.[29] The reason could be the longer precursor residence time than in flow-type reactors.

Flow-type reactors are usually operated at constant pressure and precursors are pulsed into the carrier gas. Flow-type ALD reactors are closely related to CVD reactors. In flow-type reactors the cycle times can be shortened which increases the productivity which is especially important from the industrial point of view. Flow-type reactors are at the moment also more popular in research. Due to these reasons, this thesis will concentrate on the processes operated in flow-type reactors.

Many chemically different kinds of materials have been grown by ALD such as: oxides, nitrides, sulfides, fluorides and elements. Usually ALD reactions have been thermally activated but photon[30] and increasingly radical enhancement[31-36] have also been used. Several reviews on ALD have been published over the years.[17,18,20-23,37] Recently a very comprehensive review has been published.[16]

ALD is a very promising deposition method for future microelectronic components. The excellent conformality, accurate thickness control down to nanometer level, and uniform film properties over large areas are the driving forces for implementing ALD in the semiconductor industry. The main drawback of ALD i.e. the slow growth rate will not cause problems anymore because the films will be so thin that most of the processing time will anyhow be consumed in wafer transportation, heating, and cooling. ALD of Al_2O_3 has

been demonstrated to work in DRAMs.[38] In addition, ZrO_2 or HfO_2 will most probably be used as a gate oxide material in MOSFETs by the end of 2004.[39]

3. Growth and Materials Properties of Selected Metal Oxides

This thesis concentrates on Al_2O_3, TiO_2, ZrO_2, $ZrTiO_4$, and $SrTiO_3$ ALD processes. They are all high permittivity materials and therefore studied as insulators in various applications such as gate oxides,[2] DRAMs,[38] and thin film electroluminescence (TFEL) displays.[40] In addition to these applications, TiO_2, Al_2O_3, and ZrO_2 are widely used as catalysts.[41,42]

In addition to the growth studies, interest in modeling of ALD growth has also been rising recently.[43-47] However, at the moment these studies have concentrated on already well known processes such as $ZrCl_4$ - H_2O [46, 47] and therefore completely new aspects have not risen from that field yet. However, when computer models and calculation power are increased, modeling will be an even more handy tool for screening new chemistries and as well as giving a detailed understanding of the already known processes.

3.1 Al_2O_3

Al_2O_3 thin films have a high band gap (~ 9eV) and high breakdown strength (6-8 MV/cm),[6] which makes them good insulators.[2] In addition, their chemical and thermal stability is good.[23] Ion diffusion in Al_2O_3 is also virtually negligible.[48] Due to these excellent properties Al_2O_3 thin films have been used and examined in TFEL displays and DRAM applications as dielectric layers and diffusion barriers.[23,48] One advantage of Al_2O_3 is that it can be deposited on silicon without an interfacial SiO_2 layer,[I,49-53] which is often easily formed and reduces the total capacitance. This is especially important when very small EOT are needed. However, in future generation DRAM and MOSFET applications pure Al_2O_3 can hardly be used due to its moderate permittivity (e_r ~ 9). Most probably it will be used as a thin buffer layer between a higher permittivity oxide and silicon.

Al_2O_3 thin films have been grown using various methods such as reactive magnetron sputtering,[54] MBE,[51] sol-gel,[55,56] spray pyrolysis,[57-59] pulsed plasma deposition,[60] ionized beam deposition,[61] and CVD.[62-66] Various precursor combinations have been used in the CVD studies.[65,66] However, the $AlCl_3$ - H_2 - CO_2 process is probably the most widely used industrially.[62] Hydrogen and carbon dioxide have been used instead of water because water would be too reactive in CVD towards $AlCl_3$ causing gas phase reactions and producing particles and non-uniform films. The process is usually catalyzed with H_2S, but PCl_3, COS and PH_3 [62] have also been used. H_2S increases the growth rate and improves the uniformity of the films.[62]

Al_2O_3 thin films have been grown by ALD using $AlCl_3$, [I,19,67,68] $Al(OC_2H_5)_3$,[67] $Al(OCH(CH_3)_2)_3$,[I] $Al(CH_3)_2Cl$,[69] and $Al(CH_3)_3$.[24,49,50,70-73] The oxygen source has been water,[19,67] hydrogen peroxide (H_2O_2),[72] oxygen,[68] or different alcohols.[67] Plasma assisted ALD has also been used. In plasma assisted ALD aluminum was first deposited from $(CH_3)_2(C_2H_5)N{:}AlH_3$ and hydrogen radicals and then the film was oxidized with oxygen radicals.[33] An ideal example of an ALD processes is the growth of Al_2O_3 from $Al(CH_3)_3$ and water. In this process, full completion of the surface reactions during each precursor pulse is observed and the reaction byproduct i.e. methane does not participate in further

reactions. Therefore, uniform film thickness and composition over large areas and deep trenches are obtained.[24] For these reasons the reaction mechanism of this process has been examined quite thoroughly especially on high surface area substrates.[70,71,74] The *in situ* studies will be presented in Chapter 6.5.1.

3.2 TiO_2 and ZrO_2

TiO_2 thin films are possible candidates for microelectronic and optical applications, photovoltaic solar cells,[75,76] and photocatalytic devices.[77-79] TiO_2 thin films have been grown using various methods such as evaporation,[80] DC magnetron sputtering,[81] sol-gel,[56,82,83] CVD,[84-87] and PECVD.[88] The easily forming oxygen vacancies can be filled afterwards by annealing in oxygen at 400 - 900 ^oC or with oxygen radicals at 200 - 500 ^oC.[80]

TiO_2 thin films have been grown using ALD from such precursors as $TiCl_4$,[89-95] TiI_4,[96-99] $Ti(OC_2H_5)_4$,[100,101] and $Ti(OCH(CH_3)_2)_4$.[102,103] The oxygen source has usually been water but hydrogen peroxide[96-98,103] and oxygen[99] have been applied too. TiO_2 thin films grown by ALD have high refractive indexes (n(580 nm) ~ 2.6),[89,90,100,102] but they suffer from low resistivity, which is apparently due to oxygen deficiency, and is also characteristic of TiO_2 films prepared using other methods.

ZrO_2 is a refractory material with a melting point of 2700 ^oC.[104] Due to the high diffusivity of oxygen it can be used in oxygen sensors. ZrO_2 thin films are also possible candidates for gate oxides.[105,106] ZrO_2 thin films have been grown using various methods such as EBE,[107] sputtering,[108] sol-gel,[109,110] CVD,[108,111-113] and PECVD.[114]

ZrO_2 thin films have been grown by ALD from $ZrCl_4$,[12,14,50,115-118] and ZrI_4.[119,120] Zirconium alkoxides such as $Zr(OC(CH_3)_3)_4$,[121] and $Zr(OC(CH_3)_3)_2(dmae)_2$,[122] have also been examined as precursors in ALD, but the main problem was their thermal instability. The oxygen source has usually been water, but hydrogen peroxide[118-120] has also been used. The chlorine content of the films was below 0.5 at. % in the $ZrCl_4$ - H_2O process at 500 ^oC.[117] The refractive index was 2.2 at 580 nm. The permittivities of the ZrO_2 thin films were 20 - 24.[50,119]

3.3 $SrTiO_3$

$SrTiO_3$ thin films have high permittivities and therefore they have been widely examined as dielectric materials for future generation DRAM capacitors.[7,8] $SrTiO_3$ films have been grown using various techniques such as MBE,[123,124] sputtering,[125,126] EBE,[127] pulsed laser deposition,[128] solution deposition,[129] sol-gel,[130] CVD,[131-133] and PECVD.[134]

Titanium halide precursors should be avoided in the $SrTiO_3$ and $BaTiO_3$ processes, because strontium and barium have a high tendency to form stable halides, thereby causing halide contamination of the films. Therefore, titanium alkoxides are preferred. For alkaline earth metals suitable precursors are more difficult to find. β -diketonates are the most common volatile precursors for alkaline earth metals, unfortunately they do not react with water. When a β -diketonate $Sr(thd)_2$ was used in combination with ozone, the as-deposited films were $SrCO_3$.[135] In the $SrTiO_3$ process with $Sr(thd)_2$, ozone, $Ti(OCH(CH_3)_2)_4$, and water, annealing at 700 ^oC was required to obtain crystalline $SrTiO_3$.[135]

A more reactive strontium precursor for ALD is strontium bis(tri-isopropylcyclopentadienyl) [$Sr(C_5{}^iPr_3H_2)_2$]. In combination with $Ti(OCH(CH_3)_2)_4$ and water $SrTiO_3$ films could be deposited at 250 - 325 ^oC.[136,137] At 250 ^oC the films were amorphous or only slightly crystalline, but the films grown at 325 ^oC were crystalline. The growth temperature could not be increased further due to the thermal decomposition of the titanium precursor.[136,137] Recent results[VII,138] have suggested that the thermal limit for titanium isopropoxide could be as low as 275 ^oC especially in reactors with large substrate areas or where long pulse lengths are needed.

The film stoichiometry can be controlled by either the $Sr(C_5{}^iPr_3H_2)_2$ - H_2O to $Ti(OCH(CH_3)_2)_4$ - H_2O cycle ratio or by the strontium precursor pulse length. The chemisorption of $Sr(C_5{}^iPr_3H_2)_2$ was not completely self-limiting but some decomposition appeared to take place, especially at temperatures higher than 250 ^oC.

The films contained 0.1 - 0.3 at. % of carbon and 0.4 - 1.2 at. % of hydrogen. No temperature dependence was observed, and so it was concluded that despite the obvious decomposition no significant amounts of impurities were left in the films. The hydrogen contamination was most probably from water because if the water dose was increased tenfold the hydrogen impurity content was increased to 4.3 at. %.[137] The crystallinity could be increased by increasing the temperature and also, surprisingly, by increasing the water dose.[137] The permittivity and crystallinity increased as a function of film thickness suggesting that the growth started with a less crystalline layer and later on the crystallinity increased. The recent results suggest that the crystallinity can be improved by using crystalline substrates.[139] The lattice mismatch between $SrTiO_3$ (100) and platinum (100) is only 0.3 %.[140, 141] However, platinum usually grows in (111) direction while ALD $SrTiO_3$ grows on (100) direction also on platinum (111).[139] The lattice mismatch between $SrTiO_3$ (100) and platinum (111) is large.

The electrical properties were measured using indium tin oxide (ITO)/$SrTiO_3$/Al structure. The electrodes had small work functions and thus the leakage current densities (measured at 1 V) were relatively high, i.e. $5x10^{-4}$ A/cm^2 (ITO negative) and $2x10^{-6}$ A/cm^2 (Al negative) for the highest permittivity films. The highest permittivities were obtained from the films which had nearly stoichiometric Sr/Ti ratios. The permittivities for the as-deposited and heat-treated films (1 h in air at 500 ^oC) were 120 and 180, respectively. When the Sr/Ti ratio was increased from 0.93 to 1.27 the refractive index decreased from 1.97 to 1.93 for the amorphous films grown at 250 ^oC. The optical properties of the crystalline films were more difficult to determine due to the extensive light scattering from the films. However, values of 2.0 - 2.3 were obtained and similarly to the amorphous films the refractive index depended on the Sr/Ti ratio.[137] The ALD growth mechanism of $SrTiO_3$ will be discussed in Chapter 6.5.2

3.4 Oxides Grown by Metal Alkoxide - Metal Halide Process

As stated in Chapter 2.2, new gate oxides without an interfacial SiO_2 layer are needed. Usually the oxygen source in ALD is water (H_2O), alcohol (ROH), nitrous oxide (N_2O), ozone (O_3), oxygen (O_2) or hydrogen peroxide (H_2O_2).[22] These oxygen sources easily form a thin SiO_2 layer on the silicon surface during the growth. This layer decreases the total capacitance of the gate oxide as discussed in Chapter 2.2. Therefore, a novel method of using alkoxides both as a metal and oxygen source was developed. [I, II, 142] Using this method Al_2O_3 was deposited on silicon without an interfacial SiO_2 layer.[I,53] The experimental results will concentrate on the growth of $Zr_xTi_yO_z$ thin films but Ta_2O_5 and other oxide processes will also be briefly reviewed. The growth mechanism of the $Zr_xTi_yO_z$ process will be discussed in Chapter 6.4.

3.4.1 $ZrTiO_4$

$ZrTiO_4$ thin films have been deposited using many different methods such as radio frequency[143-146] and dc magnetron sputtering,[147] and sol-gel.[148,149] However, no articles on CVD of $ZrTiO_4$ thin films appear to have been published so far. $ZrTiO_4$ thin films have a reasonably high permittivity of about 40 within a frequency range from a kilohertz to a few gigahertz.[143,147] The temperature dependence of the permittivity is small and the dielectric losses are also usually low (0.017 - 0.038 at 100 kHz).[147] Tin doping significantly improves the dc resistivity and breakdown characteristics of $ZrTiO_4$ films while having only a marginal effect on permittivity.[143,150] Due to their relatively high permittivity and small dielectric losses, $ZrTiO_4$ thin films have been studied for microwave applications such as resonators, filters, and microwave substrates.[143]

$Zr_xTi_yO_z$ thin films have been grown by ALD from titanium isopropoxide and zirconium chloride at 250 and 300 ^oC.[II] Below 250 ^oC no film growth was obtained and above 300 ^oC the thermal decomposition of the titanium isopropoxide was the limiting factor. With proper precursor pulse lengths a constant growth rate of 1.2 Å/cycle could be obtained at both 250 and 300 ^oC. The films were more uniform with shorter (0.2 s) $ZrCl_4$ pulse lengths than with longer ones, and it was suggested that the incoming $ZrCl_4$ etches TiO_2 by forming volatile $TiCl_4$:

$$ZrCl_4(g) + TiO_2(s) \rightarrow ZrO_2(s) + TiCl_4(g); \quad \Delta G(300\ ^oC) = -4.8\ kJ/mol^{151} \quad (5)$$

However, $TiCl_4$ was not observed in the reaction mechanism studies.[IX] On the other hand, the observed metal ratio was so close to the ideal ratio of Zr/(Zr+Ti) = 0.5 that the amount of $TiCl_4$ possibly formed would be very small and therefore hard to detect. In general it can be said that even if the reaction is thermodynamically favorable i.e. spontaneous, the kinetics can be so slow that the exchange reactions are virtually negligible with usual process parameters and pulse lengths.

The chloride contamination was high, i.e. above 9 at. % at 250 ^oC, and therefore the preferred growth temperature was 300 ^oC. At 300 ^oC carbon and hydrogen contents were below 0.5 at. % and the chloride content was 0.2 - 1 at. % as measured with TOF-ERDA. At 300 ^oC the films were slightly zirconium rich (Zr/(Zr+Ti) = 0.58). This was proposed to

be due to reaction 5. According to TOF-ERDA measurements the metal and oxygen contents were constant through the films.

Both at 250 and 300 °C the refractive indexes at 580 nm were around 2.3, which is relatively close to the bulk value of $ZrTiO_4$ (n(550 nm)= 2.37).[152] The films grown at 250 °C were amorphous, but those grown at 300 °C already exhibited slightly crystallized orthorhombic $ZrTiO_4$ structure.[153]

The permittivities of the films, measured from the In_2O_3:Sn / $Zr_xTi_yO_z$ / Al capacitor structure were rather high (ε_r = 45 - 65 at 10 kHz) but decreased as a function of frequency. When the oxide was grown on silicon the permittivity was lower (ε_r = 35 at 10 kHz) but the frequency dependence of the permittivity was also lower. The suggested explanation for this difference between the permittivities was that a low permittivity layer grew at the beginning of the deposition. This layer was proposed, although not proven, to be an amorphous $Zr_xSi_yO_z$ layer.**II** The hysteresis in the C-V curve was below 80 - 100 mV at -1.1 V, which was relatively small. It was even smaller at higher frequencies. The hysteresis should be as small as possible; otherwise the on and off voltages of the transistor would be different. The sputter deposited $ZrTiO_4$ thin films had very low dielectric losses i.e. in the order of 0.017 - 0.038 at 100 kHz and the frequency dependence of the permittivity was also small up to few gigahertz.[143,147] However, the ALD grown thin films had relatively high dissipation factors, which are directly proportional to the dielectric loss, and they depended quite heavily on the frequency used. **II** As is typical for high permittivity materials, which have relatively small band gaps and also often show tendency towards oxygen deficiency, the dc leakage currents were quite high (10^{-4} A/cm^2 at 0.2 MV/cm).**II** In a conclusion it can be said that the $Zr_xTi_yO_z$ ALD process looks promising but a lot of work has to be done to improve the electrical properties of the resulting material.

3.4.2 Ta_2O_5

The idea of using alkoxides as an oxygen source has also been used to deposit Ta_2O_5 thin films by using $TaCl_5$ and $Ta(OC_2H_5)_5$ as precursors at 275 and 325 °C.**I**,[142] The growth temperatures were relatively high for ALD because $Ta(OC_2H_5)_5$ already starts to decompose above 275 °C,[154,155] and on the other hand $TaCl_5$ starts to etch Ta_2O_5 film above 250 °C.[156]

If $TaCl_5$ was pulsed first, the films were thicker at the trailing edge. On the other hand, if $Ta(OC_2H_5)_5$ was pulsed first the thickness profile was inverted.[142] It was suggested[142] that $TaCl_5$ etches the Ta_2O_5 film although the etching should have been slow at the temperatures used.[156] At 275 °C both the growth rate and thickness non-uniformity increased as the $Ta(OC_2H_5)_5$ pulse length was increased from 0.7 to 1.0 s. On the other hand, at 325 °C the growth rate stayed at a constant level when the $Ta(OC_2H_5)_5$ pulse length was increased from 0.7 to 1.0 s. However, with pulse lengths above 1.4 s the growth rate increased rapidly.

The chlorine content significantly decreased from 6 to 2 at. % when the temperature was raised from 275 to 325 °C. The precursor pulse lengths had no effect on the chlorine contents. The hydrogen and carbon contents were below 1 at. % in each film. The electrical properties were comparable to those observed in water free processes as well as to the $Ta(OC_2H_5)_5$ - H_2O [155,157,158] and $TaCl_5$ - H_2O processes.[18,155]

3.4.3 Other Oxides

The new chemistry, where alkoxides were used as oxygen source, was found to be very versatile. Many precursor combinations were successful (see Ref. **I** Table 1). A couple of general trends can be found. As compared to primary alkoxides, secondary alkoxides reacted at lower temperatures and the films contained less impurities i.e. the reactions came closer to completion. As the number of carbon bonds to the central carbon increases the stability of the cleaving carbocation also increases favoring the reaction. In most cases the second precursor was a metal chloride. The electronegative chlorine most probably assists this nucleophilic attack reaction. Fluorides are more electronegative than chlorides and therefore it would be interesting to see if they would be even more reactive towards the alkoxide group. On the other hand, the metal - iodine bond is usually weaker than the other metal - halide bonds and therefore metal iodides might produce films with less contamination.

SiO_2 growth experiments using the silicon alkoxide - silicon chloride approach were unsuccessful. In the sol - gel experiments it was found that SiO_2 was obtained from primary or secondary alkoxides only when a metal catalyst was used.[159] SiO_2 thin film growth has always been difficult with ALD, the growth rate has been very low,[26,28] the needed precursor pulse lengths have been relatively long,[26,28] or the film growth has stopped after a couple of hundred cycles.[160] However, recently SiO_2 growth has been reported to occur by using silane, siloxane or silazane as silicon and ozone as oxygen sources.[161]

Zirconium silicate growth was successful.[**I**] It was the first time that silicon could be incorporated into the ALD grown films with pulse duration in the order of seconds using a flow-type reactor. However, recently metal silicates have also been grown successfully by using metal amides and tris(alkoxy)silanols as precursors.[162]

The films grown by the metal alkoxide - metal halide approach usually contained above 1 at. % of chlorine which may be too much for materials to be used in semiconductor applications. Chlorine can have serious effects on the operation of devices and the lifetime predictions of the components may be difficult to make. In our experiments the film had uniform composition throughout the whole film. However, the metal ratio did not always follow the metal precursor pulsing ratio. One possible explanation could be the metal exchange reaction (Eq. 5, see also Ch. 6.2.3). [**I, II**]

4. *In Situ* Characterization Methods for Atomic Layer Deposition

4.1 General Requirements

This thesis concentrates on the flow-type reactors as already discussed in Chapter 2.3. A couple of requirements have to be fulfilled when choosing an *in situ* characterization method for a flow-type ALD reactor. The process temperatures are usually 200 - 500 ^{o}C.[16] The amount of reaction byproducts is relatively low because only about 10^{14} molecules are released per cm^2. In addition, the ALD reactions are usually relatively rapid and therefore fast and sensitive *in situ* characterization methods are needed.

Ultra high vacuum (UHV) methods such as XPS, LEIS, AES, SIMS, RHEED and LEED have been used for *in situ* monitoring of thin film growth. Flow-type ALD reactors are usually operated at about 1 - 10 mbar so UHV methods cannot be used without proper pressure reduction. Accordingly, if these methods were used in a flow-type reactor a vigorous pumping down of pressure or a separate analyzing chamber would be needed.[163] However, the surface can change during the pressure pump down or transportation, and therefore the results are not necessarily representative anymore. For these reasons UHV methods will not be discussed in this thesis. The *in situ* methods which can be used in flow-type conditions, can be divided to three groups: optical methods, microgravimetric methods, and mass spectrometry. The first two methods characterize the surface and the third the gas phase.

4.2 Optical Methods

Optical methods can be used for analyzing both the substrate surface and gas phase. The sensitivity is a major concern in both cases. Usually porous materials have been used to obtain a large enough surface area. The commonly used optical methods for ALD process monitoring are: infrared (IR) spectroscopy, reflectance difference spectroscopy (RDS), incremental dielectric reflection (IDR), and surface photoabsorption (SPA). In addition, ellipsometry has also been used.[164,165]

IR has been used to monitor CVD[133,166] and ALD processes.[164,167,168] IR can be used to follow various important processes such as the decomposition of precursors, amount of reaction byproducts released, and the precursor evaporation rate.[166] One advantage of IR spectroscopy over the other optical methods is that chemical information can be obtained. In addition, the integrated absorption peak is directly proportional to the species concentration and therefore quantitative analysis is possible.[166] Data can be acquired in almost any process conditions. However, IR adsorption coefficients have nonlinear temperature dependences[169] and therefore if quantitative results are needed the measurement chamber should be kept at a constant temperature. To avoid this problem, the IR chamber is usually kept outside the reactor at room temperature. However, for this reason radicals and other short living species cannot be detected. The sensitivity of IR spectrometers are approaching that needed for ALD studies. In general, it can be said that the disadvantages of IR spectroscopy are that measurements are relatively slow, the data is sometimes hard to interpret, and the vibration bands can overlap.

In RDS, the reflectivity differences of polarized light between two crystallographic axes of the substrate are measured. In RDS only epitaxial films can be monitored.[170] ALD oxides grow only rarely epitaxially and therefore RDS will not be discussed anymore. Methods such as IDR[171] and SPA can be used in ALD with planar substrates. In both techniques the sample is probed with p-polarized light exactly at the Brewster angle and the reflectivity changes are monitored. In IDR the change is caused by the interference effect while in SPA by light absorption. Both techniques are capable of following changes in surface termination and thereby examining the dynamics of ALD reactions. However, the limitations of these techniques are that chemical information is difficult to obtain. In IDR studies the film and surface layer have to be dielectric and transparent.[171] IDR studies have concentrated mostly on $TiCl_4$ - H_2O [95,171-173] and $SnCl_4$ - H_2O [173] ALD processes.

4.3 Mass Spectrometry

Mass spectrometry has been widely used to study CVD[174-176] and also increasingly ALD processes.[**III, V-X**, 177-179] The time of flight mass spectrometer (TOF-MS) and QMS are the main type of instruments used in the *in situ* CVD studies. QMS is usually inexpensive and compact and therefore more common.

QMS has many advantages for *in situ* ALD process monitoring: the response time can be shortened, sampling at high temperatures is possible and almost all chemicals can be studied. Disadvantages are: i) it needs a pressure reduction which decreases the sensitivity, ii) the positive ionization of some electronegative molecules such as iodine can be hard, and iii) the interpretation of mass spectra may sometimes be complicated. The operating conditions, especially the pressure, of QMS and ALD reactors are usually different and therefore QMS cannot be installed directly inside an ALD reactor.

The key aspects that should be considered when a QMS is integrated to a flow-type ALD reactor are: pressure reduction (Ch. 5.1), surface area dependence of the amount of reaction byproducts, fast pulsing, and relatively high temperatures (200 - 500 ^{o}C) that are usually needed for the ALD processes.

In ALD, in maximum a monomolecular layer reacts during each pulse, so it can be estimated that about 10^{14} molecules are produced per one square centimeter. That is why the surface area of the substrates should be large. However, to maintain the relevance of flow-type thin film growth reactors, porous substrates should not be used because then the pulse and purge times would need to be essentially longer. On the other hand, the ALD reactions are often very fast, and therefore the measurement time should be below 100 ms. Typical temperatures used in ALD processes are between 200 and 500 ^{o}C.[16,22] The highest operating temperature for the QMS detector and electronics is usually only 50 ^{o}C and they should be protected against high temperatures.

4.4 Quartz Crystal Microbalance

Quartz has good piezoelectric properties and therefore it has been used in many applications. One very interesting application is QCM, introduced by Sauerbrey.[180] It is widely used for mass monitoring during film growth, sorption and other surface studies in both liquid and gas environment.[181,182]

At the moment electrochemical QCM (EQCM) is frequently used for monitoring electrochemical processes.[183] It is a very powerful technique because at the same time mass changes and current can be monitored. With this information it is possible to calculate the number of electrons transferred during oxidation or reduction reaction and thus obtain information about the growth mechanism.[183] QCM has also been used as a selective molecule analyzer.[181,184,185] In this application the surface of the QCM is coated with a material which bonds selectively only to the molecules under interest. By following the mass change it is possible to calculate the number of molecules. In addition, exotic applications such as Au-Hg phase diagrams have been obtained with QCM.[186]

The power of QCM lies in its extreme sensitivity, which is typically far below one monolayer. When a certain mass is deposited on a quartz crystal the resonant frequency changes according to the equation:

$$\Delta f = -\frac{2 f_0^2 \Delta m}{A\sqrt{m r}} = -C\Delta m \qquad (6)$$

where Df is the change in the resonant frequency of a quartz crystal, f_0 the fundamental resonant frequency of the unloaded quartz, Δm the mass change, A the surface area, m the shear modulus of the AT-cut quartz ($2.947*10^{11}$ g cm^{-1}s^{-2}), r the density of quartz (2.648 g cm^{-3}), and C the crystal dependent constant.[187]

The resonant frequency of the quartz crystal not only depends on the mass change but also on the gas viscosity, stress in the forming film, pressure, and temperature.[182] However, in typical measurements where relatively thin films are deposited under constant pressure conditions, all but the temperature effect can be neglected.[188] The absolute temperature limit for the QCM measurements is the Curie temperature of quartz (573 ^{o}C) where the piezoelectric properties disappear.[189] The advantage of QCM is that it can be used over a wide pressure range i.e. from UHV to above atmospheric pressures. QCM is a powerful method for examining ALD processes *in situ* and has already been used extensively for this purpose(Table 1).

Table 1. Selected ALD processes studied *in situ*.

Material	Process	Method
SrO	$Sr(C_5H_2{}^iPr_3)_2 + D_2O$	QCM,[X] QMS[X]
	$Sr(thd)_2 + H_2O$	QCM[190]
ZnO	$Zn(C_2H_5)_2 + H_2O$	QCM,[191] IDR[192]
Al_2O_3	$AlCl_3 + H_2O$	QCM[193]
	$Al(CH_3)_3 + H_2O/ D_2O$	QCM,[V,194] QMS,[V,177] FTIR[167,168]
	$+ H_2O_2$	QCM[195]
SiO_2	$SiCl_4 + H_2O$	FTIR[167]
TiO_2	$TiCl_4 + H_2O/D_2O$	QCM,[91-94,196] QMS,[196] IDR,[95,171-173,197]
	$TiI_4 + H_2O_2$	QCM[97]
	$+ O_2$	QCM[99]
	$Ti(OC_2H_5)_4 + H_2O/ D_2O$	QMS, [VI] QCM,[101]
	$Ti(OCH(CH_3)_2)_4 + H_2O/ D_2O$	QMS,[VII,194] QCM[VII,103]
ZrO_2	$ZrCl_4 + H_2O/ D_2O$	QMS,[VIII] QCM[VIII,118]
	$ZrI_4 + H_2O$-H_2O_2	QCM[120]
HfO_2	$HfCl_4 + H_2O$	QCM[198]
	$HfI_4 + H_2O_2$	QCM[199]
SnO_2	$SnCl_4 + H_2O$	IDR[173]
V_2O_5	$VO(OCH(CH_3)_2)_3 + H_2O$	QCM[200]
Ta_2O_5	$TaCl_5 + H_2O$	QCM,[156,193,201-203] AES[204]
	$TaI_5 + H_2O$	QCM[205]
	$Ta(OC_2H_5)_5 + D_2O$	QMS[VI,194]
Nb_2O_5	$NbCl_5 + D_2O$	QMS,[206] QCM[206]
	$Nb(OC_2H_5)_5 + H_2O / D_2O$	QMS,[VI,194,206] QCM[206]
$SrTiO_3$	$Sr(C_5H_2{}^iPr_3)_2 + Ti(OCH(CH_3)_2)_4 + D_2O$	QMS,[X] QCM[X]
$ZrTiO_4$	$ZrCl_4 + Ti(OCH(CH_3)_2)_4$	QMS,[IX] QCM[IX]
SrS	$Sr(thd)_2 + H_2S$	QCM[190]
ZnS	$ZnCl_2 + H_2S$	QMS[179]
In_2S_3	$In(acac)_3 + H_2S$	QCM[207-209]
TiN	$TiCl_4 + ND_3$	QMS[210]
Ti(Al)N	$TiCl_4 + ND_3 + Al(CH_3)_3$	QMS[210]

Although the frequency change of a QCM is directly proportional to the weight change, the conversion to film thickness has many uncertainties. In the first place, the frequency is not only affected by the weight change but also by gas viscosity, stress in the forming film, pressure, and temperature.[182] In addition, the density of the film is usually not constant as a function of temperature, which would therefore affect also the estimated thickness. Due to these reasons we preferred to use the primary data (frequencies), which is adequate for the reaction mechanism studies. The growth rates obtained in arbitrary units can be compared to the growth rates obtained from the thin film growth experiments by normalizing the growth rates according to one temperature.

4.5 Information Obtained from the QCM and QMS Data

General Experimental Aspects. The starting surface can have an effect on the growth rate and mechanism. It is common practice to grow 30 - 50 cycles of the corresponding material on the substrates before each experimental set to ensure proper growth surface. On the other hand, due to this procedure the *in situ* results represent more bulk growth than the interface formation. However, the effect of different growth surfaces can be studied by growing the desired material before the actual film deposition.[X]

Surface Reactions vs. Fragmentation. D_2O was used as the oxygen source in almost all *in situ* studies in this thesis.[III, V-VIII, X] Deuterated water was used instead of normal water to distinguish, using QMS, the species coming from the surface reactions from those coming directly from the metal precursor. However, there were weak background signals in the ions arising from the deuterated ligands even when no exchange reactions should have taken place, i.e. when subsequent pulses of only one precursor were given. There are many possibilities that could cause the background signal: rearrangement reactions during the ionization, condensation of the metal precursor to the cooler end of the reactor tube behind the QMS sampling capillary or orifice, incomplete relaxation of the electronics of the QMS during the fast experiments, insufficient mass resolution of the QMS, and a pressure change during the precursor pulse which could affect the observed signal. It is unclear what was the main cause of the background signal. Anyhow, to compensate for the background, the intensities measured during the ALD process with alternate pulsing were corrected by subtracting the intensities measured during the separate precursor pulses (Fig. 4). The shaded area is the amount of reaction byproducts obtained during the ALD process. The growth rate obtained with QMS is the amount of byproducts released during both precursor pulses.

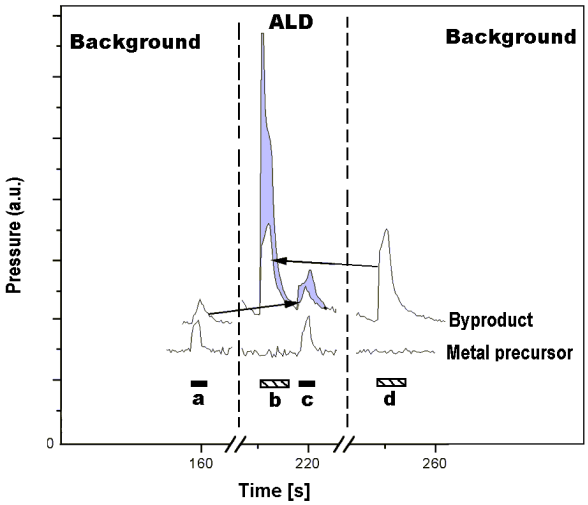

Figure 4. The background subtraction from the QMS data. a is the metal precursor pulse on the surface that is already saturated with the metal precursor. d is water pulse on the surface that is already saturated with water. b is the water and c the metal precursor pulses during ALD, respectively. The shaded area is the amount of reaction byproducts released.

QCM Data. Figure 5 a shows ideal QCM data during ALD growth from a metal precursor and water. The weight increase during the metal precursor pulse (ML_x) is labeled as m_1. During the water pulse the mass decreases because the heavier -L surface groups are replaced by -OH groups or oxide ions. The mass increment during a complete ALD cycle is m_0, which is directly related to the growth rate. As these masses are related to the adsorbates, $-ML_{x-n}$ (m_1) and MO_y (m_0), their ratio can be used to estimate how many ligands are released during the metal precursor and water pulses:

$$\frac{m_0}{m_1} = \frac{M(MO_y)}{M(ML_x) - nM(HL)} \qquad (7\text{ a})$$

$$\Leftrightarrow \qquad n = \frac{M(ML_x) - \frac{m_1}{m_0} M(MO_y)}{M(HL)} \qquad (7\text{ b})$$

Where M(*i*) is the molar mass of the species *i* and *n* is the number of ligands released during the metal precursor pulse:

$$n\text{-OH (s)} + ML_x(g) \rightarrow (\text{-O-})_n ML_{x-n}(s) + n\ HL\ (g) \qquad (8)$$

The practice adopted by us has been to calculate first *n* from the equation 7 b and then divide it by the total number of ligands in the metal precursor (*x*) to give the ratio *n* / *x*. This is practical because similar *n* / *x* values can also be calculated from QMS data by dividing the amount of reaction byproducts released during the metal precursor pulse by the total amount of reaction byproducts released during one cycle.

Overall Shape of the QCM Data. Figure 6 shows schematic growth rate behavior for different kind of ALD processes. In the middle regime (3) the reactions are saturative. This region is called the ALD window.[20] It can be very narrow or in some processes it does not exist. The growth rate and material properties can also be temperature dependent inside the ALD window. The key issue is whether the self-limiting growth is obtained during all the precursor pulses i.e. are the precursor pulses saturating the surface at a given temperature or not. If at low temperatures as the growth rate increases the temperature is lowered (1) it suggests condensation of the precursor, i.e. more than one monolayer of precursor is adsorbing. On the other hand, if the growth rate decreases (2) it suggests that the growth is kinetically limited. At high temperatures, if the growth rate increases with increased temperature (4) thermal decomposition of the precursor is likely. On the other hand, if the growth rate decreases (5) species are desorbing from the surface or the number of suitable adsorption/chemisorption sites is decreasing.

In the ideal case a fast saturation of the surface mass is obtained during each precursor pulse and the mass stays at a constant level during the purge periods (Fig. 5 a and zone 3 in Fig. 6). The mass change during the metal precursor adsorption (m_1) and the total mass change after the complete ALD cycle (m_0) depends of course on the process used. For example, m_1 can even be smaller than m_0 if ligand is very light such as methyl.[V] If the obtained QCM signal differs from the ideal case it indicates that in addition to the ALD type exchange reactions other reactions are also taking place.

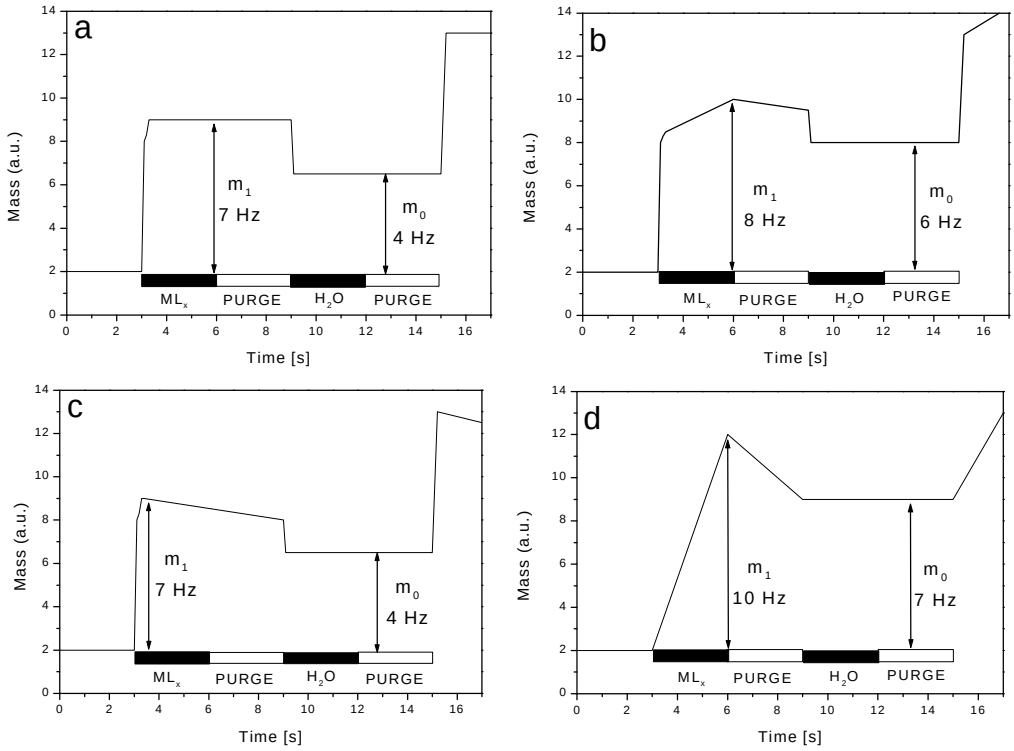

Figure 5. Schematics of QCM mass changes in different kinds of ALD processes. The examples are for oxide growth from metal precursor (ML_x) and water but in general the same kind of behavior can also be observed in other precursor systems.

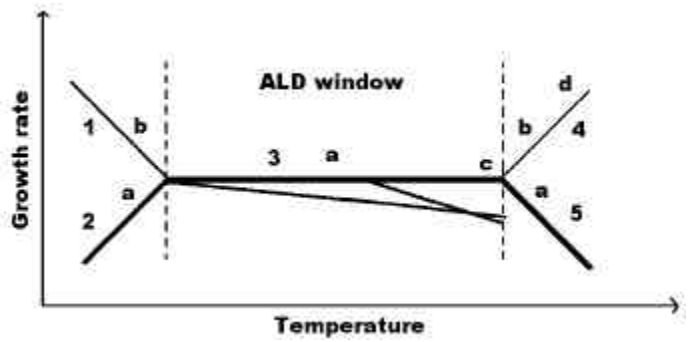

Figure 6. The growth rate as a function of temperature in different kind of ALD processes. The numbers refer to different growth regions and the letters to the QCM curves presented in Fig. 5.

If the mass does not reach the saturation level during the metal precursor pulse (Fig. 5 b) it indicates the decomposition of the precursor, inefficient precursor transportation, or slow surface reactions. Decomposition can be ruled out if m_0 saturates with long precursor pulses. The precursor transportation limitation can be ruled out by increasing the precursor flow rate. However, it should be kept in mind that the higher concentration of precursor in the gas phase can also enhance the rate of the surface reactions.

If the mass starts to decrease slowly during the metal precursor pulse and/or purge (Fig. 5 c) it indicates that the surface groups are not stable. They may recombine and desorb from the surface. However, if m_0 stays constant irrespective of the purge time after the metal pulse it indicates that only the ligands are leaving the surface and not the metal containing species. This was observed, for example, in a TiO_2 study from TiI_4 and H_2O-

H_2O_2.[97] On the other hand, if m_0 decreases as a function of the purge time it means that weakly bonded, i.e. physisorbed surface species are desorbing from the surface. Figure 5 d shows an extreme case where the precursor is decomposing rapidly and no real self-limiting growth is obtained.

Reaction Kinetics and Precursor Transportation. The reaction kinetics and precursor transportation can be studied by plotting the amount of reactions as a function of precursor pulse length.[VIII] Usually ALD reactions in a flow-type reactor are fast and completed in less than 100 ms,[211] and therefore in most cases the saturation of the surface is mass transportation limited. However, sometimes also slower processes such as opening of new adsorption sites, which have been blocked by sterical hindrances of the ligands on the surface, or other surface reconstructions may occur. This was observed for example in a ZrO_2 study from $ZrCl_4$ and water where after a rapid initial mass increment a slow saturation was observed.[VIII] In some cases the thermal decomposition of the surface groups is slow i.e. with short pulses almost ideal ALD behavior can be obtained but with long metal precursor pulses the mass starts to increase very rapidly as in the $SrTiO_3$ process.[X]

Artifacts in the QCM Data Caused by Water Pulsing. In quite many studies where the oxygen source has been water a small hump in the mass curve has been observed during the water pulse and the following purge (Fig. 7).[V, VII,190] This effect is especially strong at elevated temperatures. Interestingly with long (60 s) water pulses this hump reached a saturation level (Fig. 7 b). Also a substrate material dependence was observed.

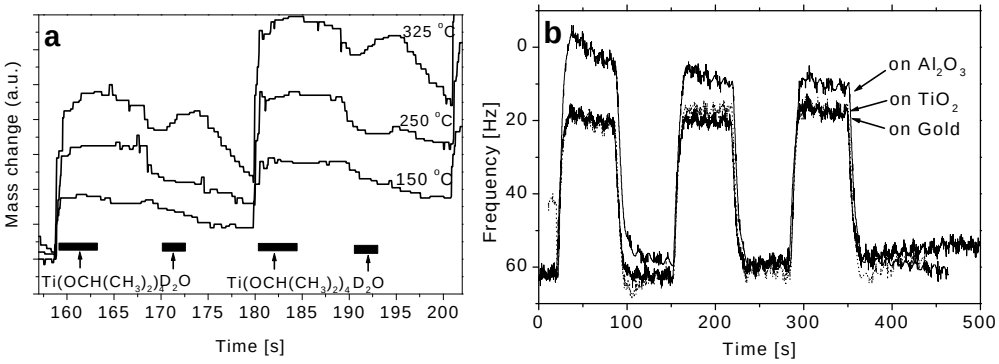

Figure 7. a) QCM mass change in two complete ALD cycles at different temperatures. The $Ti(OCH(CH_3)_2)_4$ and D_2O pulse lengths were 5 s and 2 s, respectively. The purge time was 5 s.[VII] b) The frequency change when D_2O was pulsed on Al_2O_3, TiO_2, and gold surfaces at 450 °C.

There are basically two explanations for this behavior. The first one is that the weight change was caused by the D_2O adsorption and desorption during and after the D_2O pulse, respectively. At high temperatures both processes can be pronounced which increases this effect. On the other hand, the QCM sensor is sensitive not only to the weight changes but also to temperature changes.[189,190,212] In addition, the temperature sensitivity increases as a function of temperature.[189] Therefore, the second explanation is that the D_2O pulse cools the quartz crystal and thus changes the frequency until the crystal has warmed up again.[190] The hump has been observed in our studies only with water even if the precursor such as $Al(CH_3)_3$ had a comparable vapor pressure and was fed the same way as water.[V] This suggests that the observed change in the frequency is related to the properties of water. On one hand, water adheres strongly on surfaces and on the other hand water is

an effective coolant. However, the effect can be diminished or even avoided if the crystal is turned parallel to the flow direction.

Thermal Decomposition of Precursors. Thermal decomposition of precursors as a function of temperature can best be followed with QMS by the ratio between decomposition products to the amount of precursor detected. By this procedure the precursor dose does not need to be calibrated. Also the effects of fragmentation cancel out. This is presented in Chapter 6.3.1.

The decomposition of the precursor can be studied with QCM by plotting the m_1 value as a function of precursor pulse time. If m_1 does not saturate to a constant level but increases all the time it indicates the thermal decomposition. Thermal decomposition can also be studied by plotting m_0 and n values as a function of temperature. If m_0 starts to increase rapidly when the temperature is raised it may indicate decomposition. At the same time m_0 / m_1 value usually starts to increase, which affects also the n value. This is due to the fact that as the precursor decomposes the m_0 increases but m_1-m_0 is usually constant i.e. as m_0 and m_1 increase their ratio approached unity as can be seen from Figure 5 b. The precision of the estimation for the onset of the decomposition can be improved if the growth rates obtained from the QMS and QCM data are compared. The surface can have an effect on the onset temperature for the thermal decomposition of precursors. One example is the thermal decomposition of $Sr(C_5{}^iPr_3H_2)_2$. It can decompose on oxide surfaces at around 300 ^oC,[X,137] while on sulfide surface the decomposition was moderate even at 380 ^oC.[213]

If D_2O is used instead of H_2O, the deuterated reaction byproducts can be formed only in the surface reactions with -OD groups. Therefore, the thermal decomposition of the metal precursor does not increase the amount of deuterated reaction products. This will lead to a situation where the growth rate measured with QCM increases faster than the growth rate measured with QMS, i.e. the onset of the decomposition can be obtained from the separation point.

In conclusion it can be stated that the reaction mechanisms obtained from the QMS results are more reliable because they are affected only by the ALD exchange reactions. Therefore, for example the precursor decomposition does not affect the results. In addition, in some cases desorption occurs during the purge period and therefore m_1 may be difficult to determine. On the other hand, QCM is a more reliable method for obtaining the growth rate because the size of the sampling orifice of QMS varies during the measurements as film grows on it.

5. Construction of the *In Situ* Characterization Equipment

The general aspects for choosing the *in situ* characterization methods for ALD have already been discussed in Chapters 4.1 and 4.3. This chapter concentrates on the description of the development of the *in situ* characterization system. In Chapter 5.1 the QCM - QMS system will be described and in Chapter 5.2 the improvement of the QCM method will be discussed.

5.1 QMS - QCM Set-up

The highest operating pressure of QMS is 10^{-4} mbar while ALD reactions are usually carried out at around one mbar.[22,24] Here the methods for effective pressure reduction will be discussed. One stage pressure reduction is the simplest. However, sometimes a more complicated multistage pressure reduction system is needed for example if sampling is accomplished from reactors at atmospheric pressures. The most often used pressure reduction systems are capillary,[214-216] orifice,[217] jet-separator,[218] long tube,[174,219,220] and the small controlled leak.[221] In addition, membranes, which can separate gases, have been used.[222] In all cases differential pumping is needed, i.e. the reduced pressure stage has its own pump. Turbomolecular pumps are the most popular due to the easy usage, avoidance of oil vapor contamination and low amount of maintenance needed.

Long tubes can be used only when all precursors and reaction byproducts are volatile enough so that no condensation occurs at temperatures used. This may sometimes be hard to arrange in an ALD reactor because the allowed temperature limit for the backside of the reactor is usually below 200 ^{o}C due to the rubber gaskets used for the sealing. Very fast reactions cannot be followed due to relative slow response time of a long pump line. In addition, reactions can occur in the tube. Due to these reasons, in most cases the long tube is not recommended as a pressure reduction system for ALD *in situ* measurements. The controlled leak and gas separating membrane are, on the other hand, technically more difficult to operate and construct than the capillary and orifice and therefore will not be discussed further.

Capillaries are inexpensive, easy to make and capillaries with different diameter are easy to find. The drawback of a capillary is that even if it can be made short still some condensation may occur on the capillary and eventually it can get stuck. In addition, the reactions occurring on the inner surface of the capillary can have an effect on the QMS results obtained. In addition, very reactive species such as radicals are usually impossible to detect by using a capillary.

Orifices are the most recommended pressure reduction systems for ALD because they are easy to use and fabricate. If the pressure after the pressure reduction is about half of the original pressure, a molecular beam is formed.[223] This means that almost all of the thermal and vibrational energies are translated to the kinetic energy and the beam will be supersonic.[224] Due to the low thermal energy almost all reactions are frozen in the beam[214,223] and therefore also very reactive species like radicals can be detected using this method.

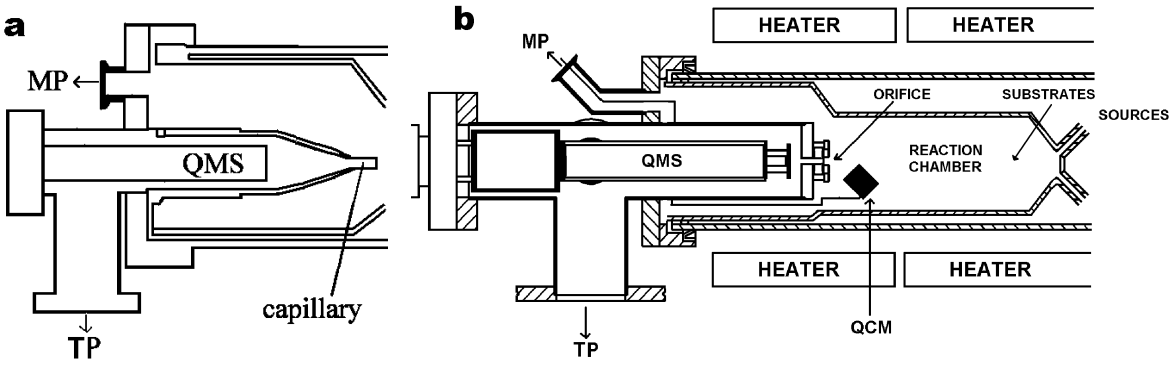

Figure 8. A schematic side view of a) the old and b) the new QMS sampling system. The precursors are transported with the carrier gas to the reaction chamber from the right and are pumped by the mechanical pump (MP). A small part of the total flow is pumped by a turbomolecular pump (TP) through a sampling capillary / orifice to the QMS chamber.

The experimental work presented in this thesis was done with two different kind of *in situ* characterization systems. In the first system[VI] (Fig. 8 a) the pressure reduction was accomplished with a small capillary. With proper design the pressure was reduced to below 10^{-4} mbar. However, because glass capillaries were used they sometimes broke down causing sudden pressure jumps, which were not good for the QMS and the turbomolecular pump. Although the surface area of the capillary was quite small, it could still contribute to the byproducts detected. On the other hand, if the temperature and material of the substrates and the capillary are the same, the reaction byproducts should be the same and therefore they should not significantly affect the results.

To avoid the difficulties described above a new pressure reduction system was designed.[II] In the new system the pressure was reduced by a 20 - 200 µm diameter orifice (Fig. 8 b). It had many benefits in comparison to capillary sampling. Lower pressures were easier to accomplish and as the whole system and orifice plate was made of metal, it was much easier to clean and more durable than the capillary system. In addition to the new pressure reduction system, a new QMS was also installed. The new QMS had a larger mass range (1-510 vs. 1-200) and variable ionization energy (0-150 eV), which is very useful especially when radicals are to be detected. The appearance potentials of radicals and neutral molecules are different, and therefore when mass spectra are measured below the appearance potential of neutral molecules the radicals can be separated from the neutrals.[224] In addition to Faraday detector the new QMS had also an electron multiplier detector which allowed far smaller amounts of molecules to be detected.

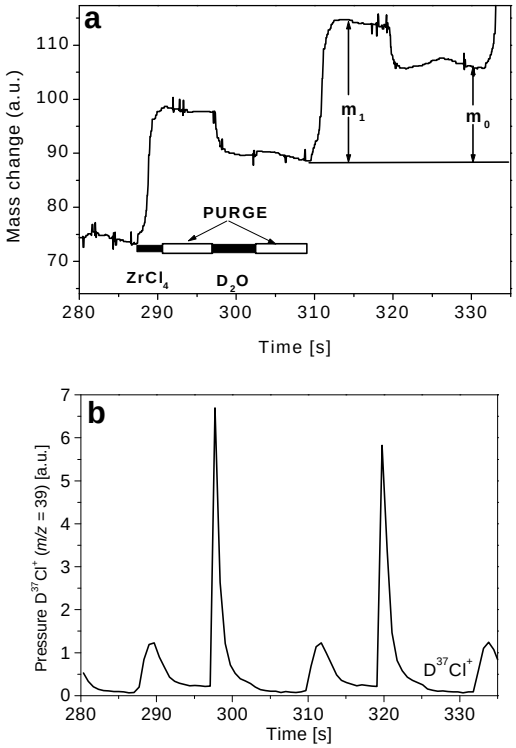

Figure 9. a) QCM mass change and b) QMS data in two complete ALD cycles at 300 °C. In a) m_0 is the mass change during one complete ALD cycle and m_1 is the mass increment during the $ZrCl_4$ pulse. $ZrCl_4$ and D_2O pulse times were 3 and 5 s and purge times 6 s, respectively.[VIII]

Figure 9 shows an example of QCM and QMS data from a $ZrCl_4$ - D_2O process. [VIII] The QCM data nicely follows the overall shape of a well-behaving ALD process presented in Chapter 4.5. During the $ZrCl_4$ pulse a mass increase (m_1) can be observed due to the chemisorption of the precursor. During the purge the mass stays at a constant level, i.e. the surface groups are stable. During the water pulse the mass decreases, which is due to the exchange reaction, where chloride ligands are changed to the lighter hydroxyl groups. The weight increase after the complete ALD cycle is labeled as m_0.

Simultaneously to the QCM measurements the process was also monitored with QMS (Fig. 9 b). During the $ZrCl_4$ pulse DCl is observed, which is formed in the surface reaction between zirconium chloride and hydroxyl groups. The signal drops to the background level during the purge. During the water pulse DCl is again observed when surface chloride groups are converted to hydroxyl groups. The signal drops to the background level as it did after the $ZrCl_4$ pulse. The ZrO_2 process will be discussed in more detail in Chapter 6.2.2.

5.2 Temperature Compensation in the QCM Method

The temperature sensitivity is the main disadvantage of the QCM method. There are basically two different ways to eliminate the temperature effect: compensation by using reference crystal and background modeling. These two techniques will be presented next.

Compensation by Using the Reference Crystal. The basic idea behind this technique is simple. When two identical crystals are compared in a way that the film can only grow onto one of these crystals, all other physical effects but the film growth can be cancelled out.[225] This technique was already used in the 60s[225] to study PVD growth and later on in CVD[182,212] and ALD studies.[IV, VIII] The corrected signal (see Fig. 1 in ref. **IV**) stayed at constant level when no growth occurred. During the ALD growth the signal rose like it should. The data was in consistency with the data obtained at lower temperature without the compensation. This proved that the method was working.

Compensation by Using the Modeled Baseline. The frequency change caused by the temperature drift can be expressed by a third order function.[212] However, it was noted that in practice a second order function is adequate.[IV] The data was fitted by using the least square method.[226] The data points (x_i, y_i) were first inserted in the matrix:

$$A = \begin{bmatrix} n & \sum x_i & \sum x_i^2 & \sum y_i \\ \sum x_i & \sum x_i^2 & \sum x_i^3 & \sum x_i y_i \\ \sum x_i^2 & \sum x_i^3 & \sum x_i^4 & \sum x_i^2 y_i \end{bmatrix} \qquad (9)$$

where n refers to the number of data points.

The matrix was resolved using the Gaussian elimination method. In this method two operations are repeatively used. One is that each line of the matrix is divided by a constant. The other operation is that each line is subtracted by another line in the matrix. When these operations are made in a proper order a matrix B is obtained:

$$B = \begin{bmatrix} 1 & 0 & 0 & b_0 \\ 0 & 1 & 0 & b_1 \\ 0 & 0 & 1 & b_2 \end{bmatrix} \qquad (10)$$

where b_0, b_1 and b_2 are the constants in the function $y = b_0 + b_1x + b_2x^2$.

The data points before and after the growth follow a function $f(x)$ and after $f(x) + A$, respectively, where A is the vertical shift caused by the film growth. The value of A was obtained by making iterations until the mean error approached a constant value. The mean error is the difference between the measured (y_i) and calculated data ($f(x_i')$):

$$S = \frac{1}{i}\sum_{1}^{i} \left| y_i - f(x_i') \right| \qquad (11)$$

Figure 2 in reference **IV** shows the temperature corrected QCM signal by using the modeling. The signals before and after the growth stayed at constant level and went up during the ALD growth. The data resembles the data obtained from a well temperature

stabilized system and therefore it can be said that the temperature effect was successfully eliminated.

When these two methods were compared it was observed that the overall shape was the same but the final level was different.[IV] Many reasons were suggested as the cause of the difference. For example, in the reference crystal method two separate crystals are used and therefore there can be a slight difference in their temperature sensitivity. It is also possible that the temperatures of the crystals change at different rates, which would make the temperature correction impossible. The main problem with the modeling is that if a real mass change is occurring during the baseline acquisition it will result in false behavior of the baseline. However, for example the effect of the desorption of surface species right after the growth is most probably an exponentially decreasing process and, therefore, when the baseline is measured long enough this problem can be avoided as well. In addition, modeling needs only one crystal so the crystal holder can be smaller and easier to construct. For these reasons modeling was concluded to be a better way for correcting the temperature effect.[IV]

6. Reaction Mechanisms in Oxide ALD Processes

Especially thermally activated ALD processes rely on the chosen precursor chemistry. Each precursor has its advantages and disadvantages. There are some general trends in different kinds of precursor classes and therefore the following chapters concerning the reaction mechanisms are divided according to the compound groups.

Metal Sources. Oxide ALD processes have been studied intensively over the years.[16] Several different kinds of compounds have been used as metal precursors such as: metal halides, alkoxides, organometallics, and β -diketonates. This thesis concentrates on the high permittivity materials to be used as insulators and therefore conducting oxides such as ZnO[191,192] or SnO_2 [173] will not be discussed.

Oxygen Sources. Oxygen molecule would be the simplest oxygen source. However, at normal processing temperatures (200 - 500 ^{o}C) it is not usually reactive enough towards the most often used ALD precursors. Anyhow, oxygen has proven to be a suitable precursor in the TiI_4 [99] and HfI_4 based processes.[227] On the other hand, oxygen radicals are very reactive and they have been used to grow Al_2O_3.[33] Water is a good ALD precursor because it is reactive towards many compounds such as metal halides and organometallic compounds, and thus it is the most often used oxygen source in ALD. Water converts the surface hydroxyl group terminated, which is a good surface for the adsorption of the metal precursor. The main disadvantage of water is that it can introduce hydrogen contamination to the films. In addition, it adheres strongly on surfaces and therefore especially at low temperatures the residual water may be hard to purge away from the substrates and reaction chamber surfaces. Sometimes, like with β-diketonates, water is not reactive enough and therefore more reactive oxygen source such as ozone has been used.[228,229] Ozone is a very reactive compound which decomposes easily to molecular oxygen and atomic oxygen, and therefore it is produced *in situ* with an ozone generator. Ozone has been proved to be a proper ALD precursor.[228,229] However, due to its reactivity it is more difficult to use than stable compounds. Hydrogen peroxide decomposes rapidly at elevated temperatures especially with a catalyst, to oxygen and water. If hydrogen peroxide can be delivered to the reaction chamber without a full decomposition it is more

reactive precursor than water. Like water, hydrogen peroxide is also capable of producing hydroxyl groups. However, there is again a possibility of hydrogen contamination. Nitrous oxide (N_2O) and alcohols have also been used as oxygen sources but not that extensively.[16] In the *in situ* reaction mechanism studies water has been the most dominant oxygen source although oxygen and hydrogen peroxide have also been used.

6.1 Surface Hydroxyl Groups

The surface chemistry of metal oxides has been studied intensively over the years.[230] The research on those oxides that have a strong catalytic effect on chemical processes such as ZrO_2, TiO_2, and Al_2O_3 has been especially intensive.[41,42] However, in this study only the surface properties which are relevant to the ALD oxide growth will be discussed.

Oxide surfaces have two different kinds of hydroxyl groups: terminal and bridging between two or more cations (Fig. 10 d).[231] The terminal hydroxyls can be either hydrogen bonded with each other (Fig. 10 b) or isolated (Fig. 10 a). The isolated hydroxyl groups are more resistant against dehydroxylation than the hydrogen bonded.

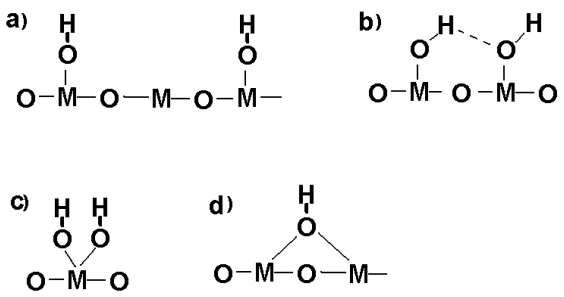

Figure 10. Different types of hydroxyl groups on metal oxide surfaces. a) Isolated terminal hydroxyl groups, b) hydrogen bonded terminal hydroxyl groups, c) geminal hydroxyl groups d) a bridging hydroxyl group between two cations.

It should be kept in mind that dehydroxylation is a continuous process. When relatively slow heating rates are used the dehydroxylation rate will be slow and therefore there will not be any significant changes in the signal. Due to this reason, a general demand for the method used is that no changes for the sensitivity as a function of temperature or time of the method are allowed. Dehydroxylation can be studied with thermogravimetry where very precise mass changes can be measured. The method was briefly tested with porous ZrO_2 and Al_2O_3 powder and it showed that the method is sensitive enough for monitoring dehydroxylation (Fig. 11). However, for obtaining quantitative results on the amount of hydroxyl groups on the surface the surface area should be known exactly. In addition, the competing adsorption of molecules other than water when exposed to air, such as CO_2, can have an impact on the results.

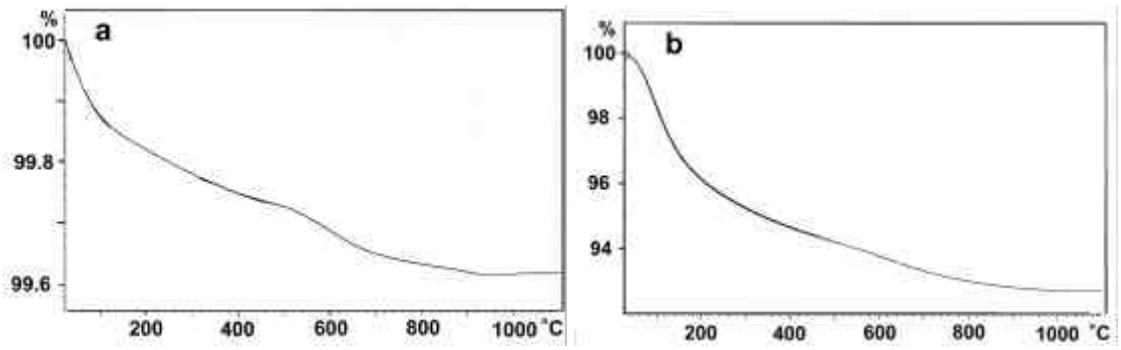

Figure 11. Mass change as a function of temperature for a) ZrO_2 and b) Al_2O_3 powder. The powders were first immersed into water over night and the water was evaporated in a vacuum for 30 min at room temperature. The surface area is not known.

QCM cannot be used for monitoring dehydroxylation because even if the temperature compensation (see Ch. 5.2) was used the signal drift caused by the temperature change would still be too high for so small mass changes. On the other hand, the sensitivity of QMS setup used in this thesis is most probably too low for the dehydroxylation measurements.

The amount and type of hydroxyl groups have been studied with IR and nuclear magnetic resonance in connection with studies where catalytic material have been modified with ALD.[41,42,71,167,232] However, to get enough signal, large surface area samples i.e. porous materials have to be used. In general, it can be stated that the problem when porous material and thin film studies are compared is that with porous materials long pulse and purge times are needed to allow the precursor molecules to diffuse inside to the smallest pores. Due to the long pulse times the material ends up in a thermodynamic equilibrium while the thin film growth is a dynamic process.

Dehydroxylation can be studied in temperature programmed desorption studies (TPD).[233,234] However, usually TPD studies are made in a high vacuum because then the mass spectrometer can be installed directly to the reactor and maximum sensitivity is obtained. The pressure difference compared to ALD processes can have an effect on the amount of hydroxyl groups on the surface. In addition, the TPD studies are usually slow and therefore the results are not necessarily representing the surface during thin film growth.

The density and the thermal stability of different hydroxyl groups vary in different materials. Agron et al.[235] have shown that the Zr-OH surface is relatively resistant against dehydroxylation while the dehydroxylation of Al_2O_3 surface depends almost linearly on the temperature.[232,233,236] The ALD growth rate can be almost constant over a quite wide temperature region.[V, VI, VII] This is somewhat surprising because the amount of active surface adsorption sites diminish at higher temperatures. The reason might be that at higher temperatures the reactions have more thermal energy and therefore also reactions with higher activation energy can occur. In addition, thermal decomposition can increase the growth rate. It should be kept in mind that even if the growth rate is constant the material properties such as impurity content, crystallinity, density, optical and electrical properties might also be changing as a function of temperature inside the ALD window.

Hydroxyl groups have usually been identified as reactive sites in ALD oxide growth.[V,22,23,41,177,237,238] The amount of hydroxyl groups has been observed to also have an impact on the growth rate and the reaction mechanism.[V,177] Almost all water and hydrogen

peroxide based ALD processes have been observed to occur at least partly through hydroxyl groups. Most of those occur even solely through -OH groups. Therefore, the presence, nature and amount of the -OH groups are very important for the growth. In some cases, especially with chlorides, the reaction mechanism seems to change as a function of temperature as the amount of hydroxyl groups decreases.

At low temperature the hydrogen impurity content is high in many water based ALD processes. This suggests that the oncoming metal precursor cannot consume all the hydroxyl groups on the surface. This can be explained by the sterical effects i.e. a part of the hydroxyl groups are covered by the bulky ligands preventing other metal precursors reacting with them. This causes a part of the hydroxyl groups to be buried in the film. Another explanation is that at low temperatures the metal precursor does not have thermal energy enough to react with all kinds of hydroxyl groups i.e. at low temperature not only the total amount of hydroxyl groups but also the nature of them can be important. Unfortunately there is no direct way to affect the nature of hydroxyl groups at constant temperature.

At high temperatures the growth rate decreases in many ALD oxide processes. The decrease can be attributed relatively directly to the decrease in the total amount of hydroxyl groups. In conclusion it can be stated that in many processes the hydroxyl groups are the reaction limiting factor.

6.2 Metal Halide Based Processes

Metal halides are good ALD precursors due to their high resistance against thermal decomposition. For example $ZrCl_4$ decomposes only above 800 ^oC.[239] Metal halides are usually very reactive towards water i.e. the ΔG is negative (e.g. for reaction $ZrCl_4 + 2H_2O \rightarrow ZrO_2 + 4HCl$; $\Delta G(300\ ^oC) = -144$ kJ /mol[151]). Metal chlorides are more common ALD precursors than metal iodides due to their higher vapor pressure (Fig. 12 a). On the other hand, in the case of zirconium and hafnium according to thermodynamic calculations[151] the iodides are more reactive towards water than chlorides (Fig. 12 b).

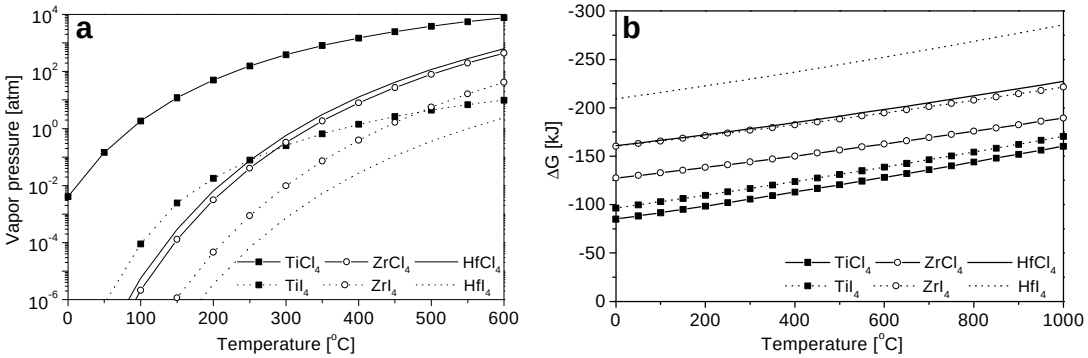

Figure 12. a) Vapor pressures and b) ΔG values for selected Group 4 halides as a function of temperature. The ΔG values have been calculated[151] for reaction $MX_4(g) + 2H_2O(g) \rightarrow MO_2(s) + 4\ HX(g)$, where M = Ti, Zr or Hf and X = Cl or I.

The main drawback of chloride precursors is halide contamination, which can cause serious problems to the device operation. In addition, the reaction byproduct with water is HCl, which is corrosive and thus sets demands for the reactor design. Due to these reasons recently metal iodides have also been studied quite intensively.[96-98,119,120,205] The metal

iodine bond is weaker than the metal chloride bond and therefore the halide contamination is usually lower with the iodides. In addition, oxygen can be used as an oxygen source in the iodide process and therefore hydrogen contamination can be avoided. On the other hand, metal iodide surfaces are not as stable as metal chloride.

The amount of -OH groups on the surface usually has a major impact on the reaction mechanism in the metal halide based ALD processes. At low temperatures when there are a lot of hydroxyl groups on the surface the incoming metal halide usually reacts with several -OH groups, while at high temperatures there are less active sites to react and thus most of the ligands are released during the water pulse.

6.2.1 $TiCl_4$ Based Process

Titanium chloride - water is a good and well-studied ALD process.[91-95,171-173,178,197,196] Many different reaction byproducts, such as Cl_2, $Ti(OH)_xCl_y$, TiO_xCl_y, have been proposed but not found. The only volatile reaction byproduct found was hydrogen chloride (DCl).[196] At low temperatures (150 ^oC) the growth occurs through two -OH groups:[196]

$$2\ \text{-OH(s)} + TiCl_4(g) \rightarrow (\text{-O-})_2TiCl_2(s) + 2HCl(g) \qquad (12\ a)$$

$$(\text{-O-})_2TiCl_2(s) + 2H_2O(g) \rightarrow (\text{-O-})_2Ti(OH)_2(s) + 2HCl(g) \qquad (12\ b)$$

In this mechanism titanium chloride reacts with hydroxyl groups and hydrogen chloride is released. During the water pulse the two remaining chloride surface groups react with water forming volatile hydrogen chloride and surface hydroxyl groups. At higher temperatures (above 350 ^oC) the reaction mechanism is changing to a direction where the incoming metal precursor reacts with only one hydroxyl group:[196]

$$\text{-OH(s)} + TiCl_4(g) \rightarrow (\text{-O-})TiCl_3(s) + HCl(g) \qquad (13\ a)$$

$$(\text{-O-})TiCl_3(s) + 2H_2O(g) \rightarrow (\text{-O-})_2Ti(OH)(s) + 3HCl(g) \qquad (13\ b)$$

The reaction 13 b can be suggested to occur in two steps where in the first step HCl is released:

$$(\text{-O-})TiCl_3(s) + 3H_2O(g) \rightarrow (\text{-O-})Ti(OH)_3(s) + 3HCl(g) \qquad (14\ a)$$

and in the second step surface dehydroxylates:

$$(\text{-O-})Ti(OH)_3(s) \rightarrow (\text{-O-})_2Ti(OH)(s) + H_2O(g) \qquad (14\ b)$$

Now the amount of hydroxyl groups is the same as before the ALD cycle. This is in line with the experimental results where each cycle was identical.[196]

6.2.2 $ZrCl_4$ Based Process

Growth Rate. The only reaction byproduct in the $ZrCl_4$ - D_2O process was DCl.[VIII] According to QMS, the growth rate increased when the temperature was raised from 250 to 300 °C (Fig. 13). On the other hand, the growth rate measured with QCM stayed at quite a constant level. The increase was explained by different surface sites.[VIII] The film growth is usually faster at kinks and steps due to the possibility to make more bonds to the surface and therefore to allow the surface to relax to smaller surface energy.[240] According to the ZrO_2 thin film growth experiments[118] the films grown at low temperatures had higher amounts of impurities. The chlorine impurity contents were 2 and 0.6 at. % at 230 °C and 300 °C, respectively. Therefore, it was suggested that a part of the precursor molecules would form a $ZrO_{2-(x+y)/2}Cl_x(OD)_y$ surface complex at low temperatures.[VIII] This complex might explain why according to QCM the mass seemed to increase at low temperatures but with QMS not that much reaction byproducts were observed. However, the difference in growth rates between these two methods was larger than the chlorine contents from the thin film growth would suggest. However, at low temperatures this process is not well established and therefore the different reactor designs can have an effect on the impurity contents and the growth rate. It is also interesting to notice that the $ZrCl_x(OH)_y$ complex has been proposed as the reason for ZrO_2 thin film agglomeration.[41,116]

The growth rate had a maximum at 300 - 325 °C after which it started to decrease (Fig 13). This decrease can be attributed to the decrease of the number of hydroxyl groups. From 350 to 500 °C the growth rate was almost constant. When the normalized growth rates are compared the growth rate in our study at 300 °C had a maximum measured both with QMS and QCM (Fig. 13 a). Otherwise the overall growth rate behavior was quite the same as what has been observed in an earlier *in situ* study (Fig. 13 b).[118]

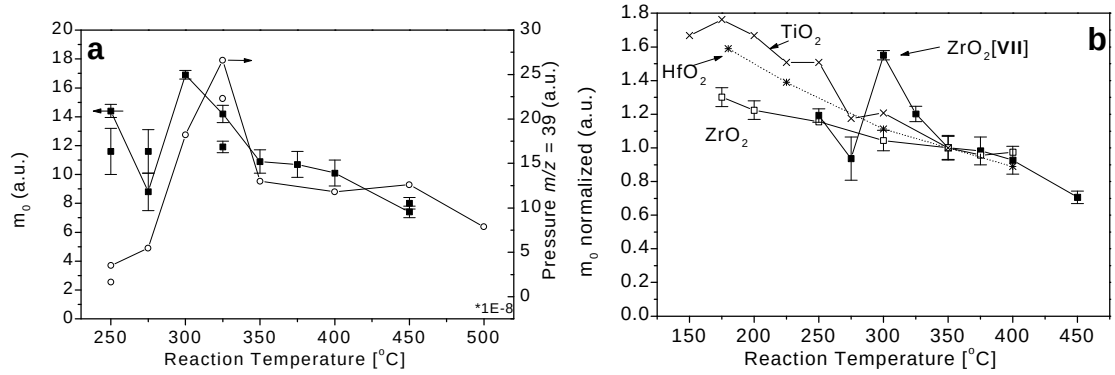

Figure 13. a) The growth rate in the ZrO_2 process as measured with QMS (solid squares) and QCM (open circles). b) The growth rate in the Group 4. metal chloride processes as a function of temperature as measured with QCM. The growth rates were normalized in each series to give unity at 350 °C. TiO_2,[196] ZrO_2,[VIII,118] HfO_2.[198]

For comparison the growth rates for other Group 4. metal chloride based oxide processes are also presented (Fig. 13 b). The m_0 values i.e. the growth rates were normalized to enable the comparison with experiments done with different kinds of QCM. At 300 °C the growth rates were around 0.5 Å/cycle for TiO_2,[89] ZrO_2,[117] and HfO_2.[241] The general decreasing trend can be seen in all these processes. The linear decrease can be attributed to the decrease in the amount of hydroxyl groups with increasing temperature.

Growth Mechanism. Half of the ligands were released during the zirconium chloride pulse and the rest during the water pulse at 250 - 375 ^{o}C (Fig. 14). The same behavior was observed in the $TiCl_4$ [196] and $HfCl_4$ [198] processes although they were carried out at lower temperatures (Fig. 14). At higher temperatures more and more of the reaction byproducts were released during the water pulse (Fig. 14). It is interesting to notice that the $ZrCl_4$ - D_2O process[VIII] resembled $Ti(OCH(CH_3)_2)_4$ - D_2O[VII] and $Al(CH_3)_3$ - D_2O processes.[V] Although, all three metal precursors are chemically relative different. Again it seems that the decrease of hydroxyl groups is affecting each of these processes.

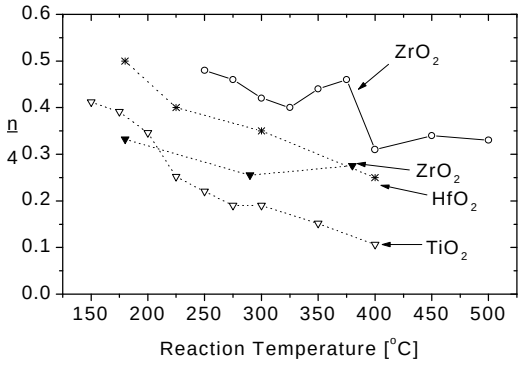

Figure 14. The fraction of chloro ligands (*n*/4) released during the metal precursor pulse as a function of temperature in Group 4 oxide processes. The *n*/4 values were calculated from the QMS data for the ZrO_2 (open circles, solid line).[VIII] The *n*/4 values for ZrO_2 (solid triangles, dotted line),[118] HfO_2 (stars, dotted line),[198] and TiO_2 (open triangles, dotted line)[196] were calculated from the QCM data.[VIII]

6.2.3 Side Reactions in the Halide Based ALD Processes

The main byproduct in chloride-based processes is usually HCl. It is a strong acid and therefore it is possible that it etches the previously grown film. There are basically two possible reaction routes. The first is that HCl forms a volatile metal halide and water:

$$MO_2(s) + 4HCl(g) \rightarrow MCl_4(g) + 2H_2O(g) \qquad (15\ a)$$

The second possibility is that the reaction byproduct is a volatile oxychloride:

$$MO_2(s) + 2HCl(g) \rightarrow MOCl_2(g) + H_2O(g) \qquad (15\ b)$$

In both cases water is formed. HCl is also usually released during the metal precursor pulse[VIII] and therefore it is possible that water is formed during the metal precursor pulse, which can cause gas phase reactions i.e. CVD type film growth. On the other hand, in some cases the oxychlorides are nonvolatile and thus can cause halide contamination.

No repeatable growth was observed in the $NbCl_5$ - H_2O process.[242] It was proposed to be due to an etching reaction:

$$Nb_2O_5(s) + 3NbCl_5(g) \rightarrow 5NbOCl_3(g) \qquad \Delta G\ (300\ ^{o}C) = -2.3\ kJ/mol^{151} \qquad (16)$$

Indeed $NbOCl_3^+$ (*m/z* = 216) was observed with QMS. When $NbCl_5$ was pulsed on a Nb_2O_5 surface a mass decrease could be observed[206] Despite the etching reaction a mass increment was observed with QCM in ALD of Nb_2O_5 from $NbCl_5$ and D_2O. It was speculated that the actual precursor in that process could be the $NbOCl_3$ that is formed in the reaction with Nb_2O_5 film coated substrates, which were located in front of the QCM. The same kind of chemistry was used in a WO_3 study where no growth was observed from WCl_6 and H_2O. However, when WCl_6 was pulsed over WO_3 powder it formed WO_xCl_{6-2x} making it possible to grow.[243]

Some surface sites can be etched faster than the other. This was observed in a TiO_2 study[95] where first a thin TiO_2 film was grown and then the surface was etched with $TiCl_4$. Due to this surface treatment a better nucleation was observed.[95] It was suggested that the amorphous phase was etched away and only the truly crystalline phase was left on the substrates.

When more than one metal is present it is possible that the film itself is not etched but the metals are exchanged:

$$TiO_2\,(s) + HfCl_4(g) \rightarrow HfO_2(s) + TiCl_4(g) \quad ;\Delta G(300\ ^oC) = -\ 73\ kJ/mol^{151} \qquad (17)$$

6.3 Metal Alkoxide Based Processes

The general formula for the binary metal alkoxides is $M(OR)_x$ and thus they can be considered as derivatives of alcohols (ROH) where the hydroxylic hydrogen has been replaced by a metal (M). The chemistry of metal alkoxides is very wide and alkoxides are known for almost every metal and also for some semimetals.[244] The chemical nature of alkoxides is significantly affected by the electropositivity of the metal and also the carbocationic nature of the organic part of the molecule (R). The organic part has an important effect on the thermal decomposition of the molecule. In metal alkoxide based processes the halide contamination and corrosive reaction byproducts can be avoided and therefore they are interesting precursors for growing oxide thin films for microelectronic applications.

Resistance against thermal decomposition is one of the most important properties of an ALD precursor. Therefore, understanding of the decomposition mechanism is a very important issue. Thermal decomposition was studied for $Ti(OCH_3)_4$, $Ti(OC_2H_5)_4$,[VI] $Ti(OCH(CH_3)_2)_4$,[VII] and $Ti(OC(CH_3)_3)_4$. In these molecules, the stability of the central carbocation increases thus weakening the titanium oxygen bond.

A characteristic feature of the alkoxide precursors is that the onset temperature for thermal decomposition is usually relatively low. The decomposition rate is slow at first but at higher temperatures it can be very fast destroying the self-limiting features of ALD. In the case of alkoxides, the decomposition product is usually the same oxide as the product of ALD exchange reactions and therefore it is sometimes hard to separate them in the growth experiments. In addition, usually CVD type decomposition at low temperatures is surface controlled so the films can be very smooth and conformal despite the decomposition of the metal precursor. Therefore, some decomposition may be acceptable in some applications.

6.3.1 Thermal Decomposition of Titanium Alkoxides

In the thin film growth experiments the thermal decomposition of ALD precursors can be studied by pulsing metal precursors onto substrates without oxygen precursors to observe whether the film grows or not. This test works on alkoxides where the oxygen is already present in the precursor molecule itself. However, even if the needed cation is present it is still unlikely that the thermal decomposition occurs at the same temperature on different surfaces.

The decomposition can be studied also by growing a film with very long precursor pulses. In ALD on porous substrates the decomposition has been observed at lower temperatures than in thin film growth experiments due to the essentially longer precursor pulse lengths needed. With long precursor pulses there is more time for the decomposition to occur and therefore also very slow reactions can have an effect on the film growth. However, even if the growth rate increases slowly with long precursor pulses it may be possible to grow thin films in an ALD kind of mode with shorter pulses.

One can also look at the deposition rate as a function of temperature. When the growth rate starts to increase rapidly it may indicate thermal decomposition of the precursor. However, it should be kept in mind that the decomposition usually starts slowly, so it is hard to observe what the real onset temperature of the decomposition is. In addition, at higher temperatures the ALD growth rate itself is usually higher due to the more thermal energy available.

In situ methods are a good way to study the thermal decomposition of the precursors. For example, in the case of titanium alkoxides the decomposition was studied by following the relative amount of a ligand fragment divided by the amount of precursor detected (Fig. 15). The detailed study of the decomposition byproducts was carried out for titanium isopropoxide only.[VII] In general, the mechanism of thermal decomposition of molecules is usually a complicated process involving several parallel and serial reactions. Fortunately, the complete decomposition mechanism is not that important for ALD growth. More important is the onset temperature of decomposition which sets the limit for self-limiting growth.

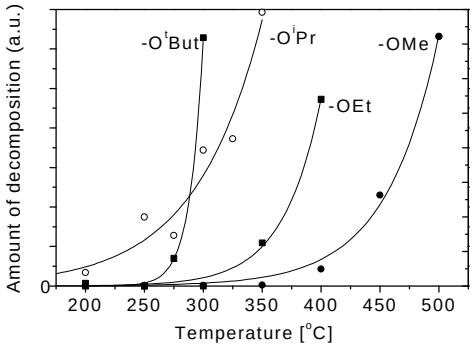

Figure 15. Thermal decomposition of $Ti(OCH_3)_4$, $Ti(OC_2H_5)_4$, $Ti(OCH(CH_3)_2)_4$ and $Ti(OC(CH_3)_3)_4$. The amount of decomposition was determined by dividing the main fragment of the ligand by a precursor fragment. The studied fragments were CH_2OH^+(*m/z* = 31) and $Ti(OCH_3)_3^+$ (*m/z* = 141) for $Ti(OCH_3)_4$, $CH_2CH_2^+$(*m/z* = 28) and $Ti(OC_2H_5)_3^+$ (*m/z* = 183) for $Ti(OC_2H_5)_4$, CH_3CHOH^+ (*m/z* = 45) and $Ti(OCH(CH_3)_2)_3(OCHCH_3)^+$ (*m/z* = 269) for $Ti(OCH(CH_3)_2)_4$ and $CH_2C(CH_3)_2^+$ (*m/z* = 56) and $TiOC(CH_3)_3^+$ (*m/z* = 121) for $Ti(OC(CH_3)_3)_4$.

The stability against thermal decomposition of titanium alkoxides increased in the order of $Ti(OCH(CH_3)_2)_4$ (225 ^oC), $Ti(OC(CH_3)_3)_4$ (250 ^oC), $Ti(OC_2H_5)_4$ (300 ^oC), and $Ti(OCH_3)_4$ (350 ^oC). It is interesting to note that the onset temperature of decomposition increases as the stability of the cleaving central carbocation decreases. The only exception is the titanium isopropoxide, which should be more resistant than titanium tert-butoxide. On the other hand, when titanium tert-butoxide starts to decompose it decomposes more rapidly than the other alkoxides studied.

Thermal decomposition has a different effect on the QMS and QCM data. In the case of titanium isopropoxide it was observed[VII] that the amount of byproducts stayed at a constant level but the mass increment per cycle i.e. m_0 increased as a function of temperature indicating the decomposition.

6.3.2 $Ti(OC_2H_5)_4$ Based Process

The only observed reaction byproduct in the $Ti(OC_2H_5)_4$ - D_2O ALD process was deuterated ethanol which was detected as $C_2H_5OD^+$ (*m/z* = 47) and CH_2OD^+ (*m/z* = 32). The CH_2OD^+ ion was more intense and therefore it was used to follow the ALD reactions. The amount of reaction byproduct had a maximum at around 300 ^oC. Therefore, the temperature range 250 - 300 ^oC was identified as the optimum growth region for this process because the surface reactions were fast enough but the decomposition of $Ti(OC_2H_5)_4$ was not yet extensive. This result was in a good agreement with the earlier growth experiments and *in situ* monitoring with QCM where the growth rate of TiO_2 was only weakly dependent on temperature in the same temperature range (biz. 250-300 ^oC).[100,101] Deuterated ethanol was observed at temperatures up to 400 ^oC in nearly as large amounts as at 250 ^oC and 300 ^oC (Fig. 6. in **VI**). This suggests that despite the thermal decomposition of the titanium precursor, the surface remains quite fully $-Ti(OC_2H_5)_{4-x}$ terminated up to temperatures as high as 350 ^oC. Therefore, it was concluded that the decomposition was surface controlled. Indeed, in earlier studies[100,101] it was found that even though the growth was not fully controlled by the exchange reactions the film thickness uniformity was not affected until above 350 ^oC.

Over 90 % of the ligands were released during the water pulse, which was suggested to be due to molecular adsorption of the titanium precursor. The second option is that ethanol produced in the exchange reactions would reabsorb on the surface and form a surface species $-Ti(CH_3CH_2OD)$ with a coordinatively unsaturated Ti atom where the bonding would be through an oxygen free electron pair:

$$-Ti + CH_3CH_2OD(g) \rightarrow -Ti(CH_3CH_2OD)(s) \qquad (18\ a)$$

It was speculated that dissociative adsorption would be even more probable:

$$-Ti + -O + CH_3CH_2OD(g) \rightarrow - Ti\text{-}O\text{-}CH_2CH_3(s) + -OD(s) \qquad (18\ b)$$

In both cases, the next D_2O pulse would release the adsorbed or dissociated CH_3CH_2OD:

$$-Ti(CH_3CH_2OD)(s) + D_2O(g) \rightarrow -Ti(D_2O)(s) + CH_3CH_2OD(g) \qquad (19\ a)$$
$$-Ti\text{-}O\text{-}CH_2CH_3(s) + D_2O(g) \rightarrow -Ti\text{-}OD(s) + CH_3CH_2OD(g) \qquad (19\ b)$$

This was tested by pulsing ethanol on a freshly grown TiO_2 surface at 250 ^oC. After a 60 s purge period water was pulsed on the surface. A mass increment during the ethanol pulse and a mass decrement during water pulse was observed. During the water pulse ethanol was observed with QMS. This proved that ethanol can adsorb on TiO_2 surface and it is therefore possible that the same mechanism affects the observed reaction mechanism during the ALD growth also. Ethanol adsorption on TiO_2 surface has been studied with IR extensively.[245] In these studies it was found that the main adsorbing species was an alkoxy group.

Quite many reaction byproducts are capable of adsorbing on surfaces during the growth. The knowledge about the adsorption of byproducts is important because the readsorption can increase the impurity contents of the films, causing a lower growth rate than in the ideal case by blocking active sites also causing nonuniform film thickness.

HCl has also been proposed to adsorb on oxide surfaces.[89,196] However, the experimental studies on TiO_2 at 250 ^oC with a flow-type ALD reactor have been unsuccessful in proving that. On the other hand, studies on the single crystal Al_2O_3 have shown that HCl is capable of adsorbing on the surface. According to TPD measurements desorption occurred over a broad temperature range of 27 - 377 ^oC.[246] The broad range suggested a distribution of surface sites with different binding energies.

6.3.3 $Ti(OCH(CH_3)_3)_4$ Based Process

The $Ti(OCH(CH_3)_3)_4$ - D_2O ALD process was studied at 150 - 350 ^oC.**[VII]** The thermal decomposition of the titanium precursor has already been discussed in Chapter 6.3.1 and ref. **VII**, and therefore in this part only the ALD reactions will be discussed. The only observed byproduct from the exchange reactions between the titanium precursor and -OD groups was $(CH_3)_2CHOD$ (*m/z* = 61), which was best resolved as CH_3CHOD (*m/z* = 46). The amount of reaction byproduct stayed at a relatively constant level from 150 to 350 ^oC. This was somewhat different than what was observed in the $Ti(OC_2H_5)_4$ based process where the amount of reaction byproduct had a maximum at about 250 - 300 ^oC. At 150 - 275 ^oC about half of the deuterated reaction byproducts formed in the ALD growth were released during the titanium precursor pulse and another half during the D_2O pulse, as calculated from QMS and QCM data. The observed reaction mechanism and its temperature dependence were quite different than in the $TiCl_4$ or $Ti(OC_2H_5)_4$ based processes. In the $TiCl_4$ - D_2O process the number of -Cl ligands released during the titanium precursor pulse decreased from two to one when the temperature was increased from 150 to 250 ^oC.[196] At higher temperatures less than one -Cl ligand was released indicating molecular adsorption of $TiCl_4$. On the other hand, in the $Ti(OC_2H_5)_4$ - D_2O process over 90 % of the reaction byproducts were detected during the D_2O pulse, which suggests that the growth occurred mostly via molecular adsorption of $Ti(OC_2H_5)_4$ and its subsequent reaction with the incoming D_2O.**[VI]**

6.3.4 Comparison of Titanium Alkoxide Processes

Figure 16 shows the fraction of ligands released during the titanium precursor adsorption in the $Ti(OC_2H_5)_4$ - H_2O/D_2O [101] and $Ti(OCH(CH_3)_2)_4$ - H_2O / D_2O processes.[VII,103]

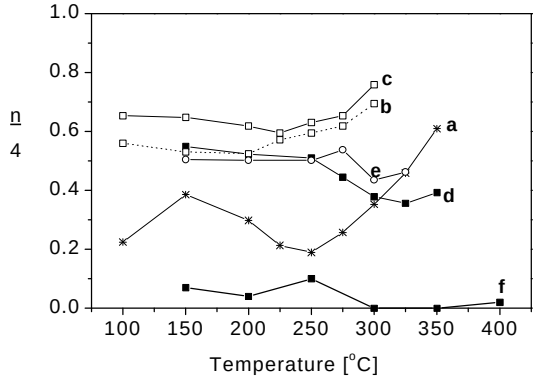

Figure 16. The proportion of ligands released during metal adsorption in $Ti(OC_2H_5)_4$ and $Ti(OCH(CH_3)_2)_4$ based ALD processes. $Ti(OC_2H_5)_4$ - H_2O process according to a) QCM[101] f) QMS, $Ti(OCH(CH_3)_2)_4$ -H_2O process[VII] b) 2 s titanium precursor pulse, QCM,[103] c) 5 s titanium precursor pulse, QCM,[103] and d) $Ti(OCH(CH_3)_2)_4$ -D_2O process according to d) QMS e) QCM.[VII]

In the titanium ethoxide based process, according to QCM measurements (curve a),[101] the *n*/4 value i.e. the amount of ligands released during metal precursor adsorption first increased from 0.2 to 0.4 and then decreased back to 0.2 as the temperature was increased from 100 to 250 °C. Above 250 °C more and more ligands were released during the titanium precursor pulse indicating thermal decomposition.[101] On the other hand, according to QMS data (curve f) the *n*/4 value was below 0.1, i.e. 90 % of the ligands were released during the water pulse between 150 and 400 °C. There is a clear difference in the results obtained between these two studies. However, in both studies it was concluded that most of the ligands were released during the water pulse. In addition, above 250 °C the difference between curves a and f is caused by the fact that the thermal decomposition does not affect the QMS results but does have an effect on the QCM results (Ch. 6.3.1).

According to QCM results, in the titanium isopropoxide study somewhat smaller amount of ligands were released during the titanium precursor pulse with shorter titanium precursor pulses.[103] Below 250 °C the results obtained by Aarik *et al.*[103] with shorter precursor pulses are in a good agreement with our results obtained both with QCM and QMS.[VII] According to QCM and QMS results, at higher temperatures the *n* value in our study was decreasing while the n value obtained by Aarik *et al.* was increasing. As already discussed in Chapter 6.3.1, the onset temperature for the thermal decomposition of titanium isopropoxide is around 225 °C. As the precursor decomposes the m_0/m_1 should approach unity, which means that the *n* value should increase. This was indeed observed in the study by Aarik *et al.*[103] However, in our study[VII] the *n* value decreased (Fig. 16, curves e and d).The general trend in many ALD processes, as already observed in the halide based processes (Fig. 14), is the decreasing *n* value as a function of temperature. It seems that there is two competing mechanisms. The *n* value is increased due to the decomposition of the titanium precursor. On the other hand the *n* value is decreased due to smaller number of hydroxyl groups on the surface. The balance between these two mechanisms can be

affected by the experimental parameters such as residence time, reactor geometry, flow rates and doses and therefore in different reactors slightly different results may be obtained.

6.3.5 $Ta(OC_2H_5)_5$ and $Nb(OC_2H_5)_5$ Based Processes

Growth Rate in the $Nb(OC_2H_5)_5$ based process. The growth rate measured with QCM increased from 150 to 300 °C after which it started to decrease.[206] The optimum growth temperature would be about 275 - 300 °C, which is somewhat higher than that observed in the thin film growth experiments i.e. 230 - 260 °C.[247] However, the difference was so small that it can very well be due to different reactor design.

Reaction Mechanism in the $Nb(OC_2H_5)_5$ based process. The main reaction byproduct in the ALD reactions was ethanol.[VI,206] At 225 °C 90 % of the reaction byproducts were released during the water pulse as measured with QMS.[206] This resembles the titanium ethoxide based process already discussed in Chapter 6.3.2.[VI] At 400 °C according to QCM the *n* value in the niobium ethoxide based process was 1 while according to QMS the *n* value was somewhat smaller i.e. 0.5. Similarly to TiO_2 surfaces[VI] the Nb_2O_5 surface was also capable of adsorbing ethanol at 250 °C.[206] The adsorption capabilities were also studied with isopropanol but it did not adsorb. The thermal decomposition of $Nb(OC_2H_5)_5$ began above 325 - 350 °C.[206] This was observed with QMS as an increasing amount of ethanol and ethane released. Diethyl ether, $O(C_2H_5)_2$, was one of the decomposition byproducts although it was also released in some extent from the ALD reactions.[VI, 206] The decomposition reaction can be proposed as:

$$2\ Nb(OC_2H_5)_5(g) \rightarrow Nb_2O_5(s) + 5\ O(C_2H_5)_2\ (g) \qquad (20)$$

It was interesting that the molecular peak of acetic acid [CH_3COOH] was also observed.[206] Indeed, carboxylate molecules were observed on the surface when ethanol was pulsed over TiO_2 surface.[245] It was suggested that ethoxide surface groups would react forming acetaldehyde which would react further with the hydroxyl group forming carboxylate molecules:[245]

$$CH_3CHO(s) + OH^-(s) \rightarrow CH_3COO^-(s) + H_2(g) \qquad (21)$$

In this reaction hydrogen is released. However, it can be suggested that at least part of the hydrogen is reacting with the surface carboxylate forming acetic acid:

$$CH_3COO^-(s) + H^+(s) \rightarrow CH_3COOH(g) \qquad (22)$$

On the other hand, acetic acid could be formed when two nearby alkoxy ligands react with each other forming acetic acid and ethane:

$$2\text{-}OC_2H_5\ (s) \rightarrow CH_3COOH\ (g) + C_2H_6(g) \qquad (23)$$

The dehydration of ethanol could lead to the formation of acetone which could react further forming acetic acid:

$$2\ CH_3CHO(g) \rightarrow CH_3COOH\ (g) + C_2H_4\ (g) \qquad (24)$$

To find out which one of the reactions is occurring the amount of ethane and ethene should be measured.

Growth Rate in the $Ta(OC_2H_5)_5$ Based Process. In film growth experiments, the growth rate increased when the temperature was raised from 150 to 225 ^oC.[155] At 225 - 325 ^oC the growth rate stayed at a constant level of 0.4 Å/cycle. Above 325 ^oC the growth rate started to decrease while above 375 ^oC it started to again increase rapidly.[155] The increase was proposed to be due to thermal decomposition of tantalum ethoxide. In another study the decomposition was observed above 275 ^oC.[154] According to QCM the growth rate increased as a function of temperature from 150 to 375 ^oC, the highest temperature measured.[154] It was proposed that two competing reactions were occurring. On one hand, the amount of reactive adsorption sites is decreasing as a function of temperature decreasing also the ALD type growth. On the other hand, the thermal decomposition of the tantalum precursor at temperatures higher than 300 ^oC increased the growth rate, i.e. the sum of these two reactions is the monotonically increasing growth rate as a function of temperature.

Growth Mechanism in the $Ta(OC_2H_5)_5$ Based Process. As expected, the tantalum ethoxide process resembled the niobium ethoxide process. In the QCM study by Kukli et al.[154] long (above 10s) tantalum precursor pulse lengths were needed to obtain steady *n* values. The *n* values were 0.5, 2.8, and 3 at 250, 325, and 375 ^oC, respectively.[154] In another QCM study the *n* value was 2 at 325 ^oC.[206] These two studies are in a relatively good agreement with each other.

In conclusion it can be said that the $Ta(OC_2H_5)_5$ - D_2O and $Nb(OC_2H_5)_5$ - D_2O processes seemed to resemble the $Ti(OC_2H_5)_4$ - D_2O process.[VI] The main difference was that during the Ta_2O_5 and Nb_2O_5 processes diethyl ether (*m/z* = 74) was observed during the metal precursor pulse at lower temperatures than in the case of TiO_2. In addition, in the Nb_2O_5 processes the total amount of CH_3CH_2OD released during the water pulse was less than in the titanium and tantalum processes. The Ta_2O_5 and Nb_2O_5 processes consists of an alternate release of $(C_2H_5)_2O$ (*m/z* = 74), during the $Ta(OC_2H_5)_5$ or $Nb(OC_2H_5)_5$ pulse, and CH_3CH_2OD(*m/z* = 47), during the D_2O pulse.

6.4 Metal Alkoxide - Metal Halide Process

The idea of using metal alkoxides as oxygen sources in ALD is new and therefore no article has been written concerning the reaction mechanism.[IX] However, the metal alkoxide - metal halide chemistry has been studied quite widely in non-hydrolytic, i.e. in absence of water, sol-gel studies. [56,248-250]

The upper limit for the $ZrCl_4$ - $Ti(OCH(CH_3)_3)_4$ ALD process is about 325 - 350 ^oC due to the thermal decomposition of the titanium precursor. On the other hand, the film properties were not good at 250 ^oC.[II] Especially the impurity contents were high as discussed in Chapter 2.4. Due to these reasons the reaction mechanism was studied extensively mainly at 300 ^oC.[IX]

The only detected reaction byproducts were HCl^+ (*m/z* = 36), $CH_2CHCH_3^+$(*m/z* = 42), and $(CH_3)_2CHCl^+$ (*m/z* = 78) and its fragment $CHCH_3Cl^+$(*m/z* = 63). According to the QMS and QCM results three out of four isopropyl ligands reacted with the zirconium chloride surface during the titanium isopropoxide pulse. The reaction which leads to a release of 2-chloropropane was suggested to be:

$$\text{-}ZrCl_3(s) + Ti(OCH(CH_3)_2)_4(g) \rightarrow \text{-}Zr(\text{-}O\text{-})_3TiOCH(CH_3)_2(s) + 3(CH_3)_2CHCl(g) \quad (25)$$

This reaction has been proposed[249, IX] to occur through a four-center transition state (Scheme 1 a) where the lone electron pair of oxygen attacks the zirconium, and the chlorine attacks the central carbon of the isopropyl group. The transition state leads to the bond breaking between zirconium and chlorine, and oxygen and carbon. At the same time new bonds are formed between zirconium and oxygen, and chlorine and carbon. The carbocationic nature of the central carbon is very important. The more stable the carbocation is, i.e. the more branched it is, the more favorable this reaction is. This was clearly seen in the thin film growth studies where secondary alkoxides were more reactive than the primary.[I]

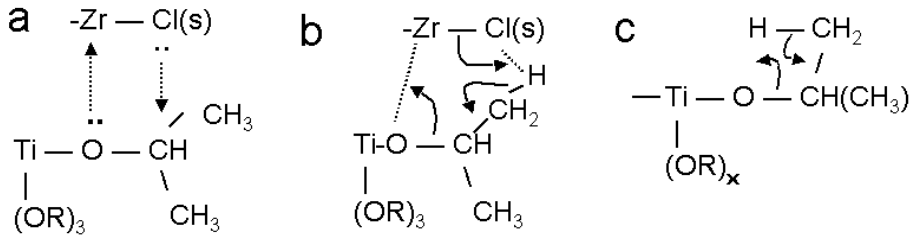

Scheme 1. a) and b) Proposed transition states between $Ti(OCH(CH_3)_3)_4$ and $ZrCl_x$ surface[IX] and c) the β -elimination reaction of $Ti(OCH(CH_3)_3)_4$.

The release of HCl and CH_2CHCH_3 was proposed to occur through a reaction:

$$\text{-}ZrCl_3(s) + Ti(OCH(CH_3)_2)_4(g) \rightarrow \text{-}Zr(\text{-}O\text{-})_3TiOCH(CH_3)_2(s) + 3CH_2CHCH_3\,(g) + 3HCl(g) \quad (26)$$

This reaction was proposed to occur through a six-member transition state (Scheme 1 b). In principle, HCl and CH_2CHCH_3 could be thermal decomposition products of 2-chloropropane. However, because 2-chloropropene was released during both precursor pulses but propene almost only (95 %) during titanium precursor pulse the decomposition was concluded not to be likely. The relative importance of the competing reactions 25 and 26 was hard or impossible to determine directly from the QCM and QMS data due to the same mass change in both reactions and, on the other hand, the different ionization efficiency of the different reaction byproducts. However, the importance between these reactions was studied by depositing first $Zr_xTi_yO_z$ by the present process, and after that ZrO_2 from $ZrCl_4$ and water. The only reaction byproduct in the ZrO_2 process was HCl[VIII] and, therefore, by comparing the amount of HCl released from these two processes it was possible to estimate how important was the reaction route, which leads to the release of HCl in the $Zr_xTi_yO_z$ process. According to this estimation 20 % of the reactions in the $Zr_xTi_yO_z$ process occur through the release of HCl. The estimation is based on an

assumption that there were equal amounts of active surface sites on the ZrO_2 and $Zr_xTi_yO_z$ surfaces. The growth rates for ZrO_2 [117] and $Zr_xTi_yO_z$ [II] are 0.53 and 1.2 Å/cycle, respectively. The growth rate per one deposited metal is about 0.6 Å/cycle and therefore the assumption proposed above is reasonable.

The four-member transition state is usually not as favorable as the six-member transition state due to sterical hindrances and more stretched bond angles from the optimal position. However, it seems that in this reaction the electronegativity difference and the lone pair electrons made the reaction 25 (Scheme 1 a) more favorable.

300 °C was already a relatively high temperature for the titanium isopropoxide and therefore it was suggested that some of the isopropoxide ligands would decompose through β-elimination producing hydroxyl groups on the surface (Scheme 1 c):[IX]

$$\text{-TiOCH(CH}_3\text{)}_2\text{(s)} \rightarrow \text{-TiOH(s)} + \text{CH}_3\text{CHCH}_2\text{ (g)} \qquad (27)$$

In addition to β-elimination an intermolecular elimination mechanism has also been proposed:[251]

$$\text{-TiOCH(CH}_3\text{)}_2\text{(s)} + \text{base} \rightarrow \text{TiO}^-\text{(s)} + [\text{HBase}]^+\text{(s)} + \text{CH}_3\text{CHCH}_2\text{(g)} \qquad (28)$$

In this mechanism a base, which could be a surface oxo or hydroxo group attacks the isopropoxide group forming protonated base and propene. At 300 °C the thermal decomposition of isopropoxy groups was proposed[VII] to be relatively slow and thus it would occur mainly during the purge period after the titanium isopropoxide pulse. Indeed, the decomposition was observed in the QCM data where the surface mass slowly decreased during the purge period after the titanium isopropoxide pulse.

According to reactions 25, 26, and 27 the surface after the titanium isopropoxide pulse contained both isopropyl and hydroxyl groups. The isopropyl groups are suggested to react with $ZrCl_4$ releasing 2-chloropropane:

$$\text{-Zr(-O-)}_3\text{TiOCH(CH}_3\text{)(s)+ZrCl}_4\text{(g)} \rightarrow \text{-Zr(-O-)}_3\text{TiOZrCl}_3\text{(s)+ (CH}_3\text{)}_2\text{CHCl(g)} \qquad (29)$$

The transition state was most probably similar to that in reaction 25 (Scheme 1 a). At the same time, zirconium chloride can also react with the hydroxyl groups releasing hydrogen chloride:

$$\text{-TiOH(s)+ ZrCl}_4\text{(g)} \rightarrow \text{-TiOZrCl}_3\text{(s)} + \text{HCl(g)} \qquad (30)$$

Both reactions 29 and 30 convert the surface to chlorine terminated and it is thus ready for the next ALD cycle.

The relative importance of HCl liberation was estimated to be 20 % of all reactions. On the other hand, according to the QMS and QCM data three out of four isopropoxide ligands reacted during the titanium precursor pulse. According to these facts a complete reaction mechanism was sketched (Scheme 2). Though other reaction pathways were found, most of the growth occurred through the release of 2-chloropropane analogous to the non-hydrolytic sol-gel processes. [56,248-250]

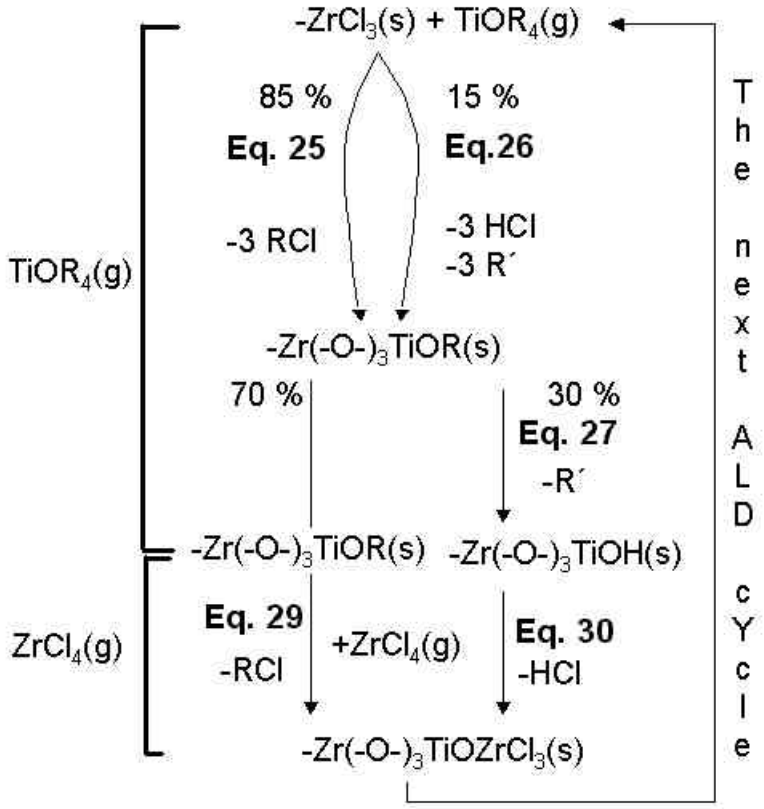

Scheme 2. A schematic overview of the reaction mechanisms in the ALD of $Zr_xTi_yO_z$ from $ZrCl_4$ and $Ti(OCH(CH_3)_2)_4$. R = $(CH_3)_2CH$, R´ = CH_3CHCH_2.[IX]

6.5 Processes Based on Organometallics

In an organometallic compound the center metal is coordinated to at least one organic group through carbon. Organometallic precursors are very common in CVD[240] and also frequently used in ALD.[16] Similar to the alkoxides, the organic group has an effect to the onset temperature of the thermal decomposition. Usually the onset temperature decreases as the number of carbon in metal alkyl increases. However, if the molecule has some favorable decomposition mechanism such as β - hydrogen elimination (Scheme 1c), the decomposition temperature can be lower than what would be expected from the carbon chain length. The vapor pressure usually decreases as the molecular weight increases. Organometallic precursors have been used in many semiconductor ALD processes such as: GaAs and silicon but those will not be discussed in this thesis.

6.5.1 $Al(CH_3)_3$ Based Process

$Al(CH_3)_3$ is one of the most ideal ALD precursors. It has a relatively high vapor pressure and the reaction byproduct with water is inert and gaseous methane. In addition, $Al(CH_3)_3$ is relatively thermal decomposition resistant. On porous materials with very long pulse times (2-6 h) thermal decomposition was observed at 370 ^oC.[71] On the other hand, in the thin film studies self-limiting growth could be obtained at 377 ^oC.[74] $Al(CH_3)_3$ has been reported to decompose at higher temperatures in vacuum into aluminum carbides.[252] Surprisingly, in the $Al(CH_3)_3$ - NO_2 ALD process[72] the growth rate increased rapidly above

300 ^{o}C indicating decomposition of one of the precursor. However, no chemical information of the films was reported. When H_2O_2 was used as an oxygen source[72] the growth rate had a maximum of about 1 Å / cycle at 250 ^{o}C above which it decreased. Above 600 ^{o}C the growth rate started to increase rapidly indicating thermal decomposition. Again no information on the films were given so it is impossible to know if some decomposition was already taking place below 600 ^{o}C. The growth rate behavior was the same when H_2O was used as an oxygen source.[178] The study also observed a maximum at 250 ^{o}C. Above that the growth rate decreased up to 500 ^{o}C, which was the highest temperature studied. In another study[73] with H_2O as an oxygen source full saturation as a function of both precursors was observed at 450 ^{o}C. According to these studies it can be concluded that with relatively short pulse lengths it seems possible to grow Al_2O_3 from $Al(CH_3)_3$ - H_2O in a self-limiting mode at least up to 450 ^{o}C.

The ALD of Al_2O_3 from $Al(CH_3)_3$ and D_2O was studied with QCM at 150 - 350 ^{o}C and with QMS at 150 - 400 ^{o}C.[V] The same process had previously already been studied with QMS.[177] However, a recent discovery[178] that the water dose, not only the pulse time, can have a significant effect on the growth rate motivated us to look at this important ALD process more closely.

***In Situ* Reaction Mechanism Studies.** In the simplest case the overall reaction between the $Al(CH_3)_3$ and water can be divided into two reactions:

$$n\text{-}OH(s) + Al(CH_3)_3(g) \rightarrow (\text{-}O\text{-})_nAl(CH_3)_{3-n}(s) + nCH_4(g) \quad (31\ a)$$

$$(\text{-}O\text{-})_nAl(CH_3)_{3-n}(s) + 3/2H_2O(g) \rightarrow \text{-}AlO_{3/2}(OH)_n(s) + (3-n)CH_4(g) \quad (31\ b)$$

During the $Al(CH_3)_3$ pulse the precursor reacts with the surface hydroxyl groups (reaction 31 a). At this stage *n* methyl groups are released. The rest of the methyl groups are released during the water pulse (reaction 31 b). After the water pulse the surface is again hydroxyl group terminated and ready for the next ALD cycle.

However, the mechanism proposed above is oversimplified because the Al_2O_3 surface after the $Al(CH_3)_3$ pulse has both methyl surface groups and coordinatively unsaturated surface (c.u.s) aluminum and oxygen sites.[74,177,237,253,254] Therefore, two kinds of reactions were suggested to occur during the subsequent water (deuterated water in that study) pulse:[V]

$$Al\text{-}CH_3(s) + D_2O(g) \rightarrow Al\text{-}OD(s) + CH_3D(g) \quad (32)$$

$$Al\text{-}O\text{-}Al\ (s) + D_2O(g) \rightarrow 2Al\text{-}OD(s) \quad (33)$$

The methyl groups bound to aluminum are very reactive towards water and the reaction 32 was proposed[V] to be very rapid with only a minor effect from the water dose. Also the c.u.s sites reacted with water forming -OD groups, but at a slower rate (reaction 33). The extent of reaction 33 can be increased by increasing the water dose.

The growth rate increased in the temperature range of 150 - 250 ^{o}C. At higher temperatures the growth rate started to decrease. The Al_2O_3 surface has different surface sites and hydroxyl groups as discussed in the Chapter 6.1. Some sites are more reactive than the others. Therefore, at low temperatures the growth rate was limited due to the kinetic reasons. At higher temperatures the growth rate was limited by the amount of surface hydroxyl groups.[V]

In an earlier study[177] it was observed that at low temperatures (150 ^{o}C) more reaction byproducts i.e. CH_3D were released during the $Al(CH_3)_3$ than during the D_2O pulse. On the other hand, at high temperatures the reaction mechanism was shifting in a direction where more reaction byproducts were released during the D_2O pulse. This was concluded to be due to dehydroxylation of the Al_2O_3 surface. However, the more recent study[V] suggested that the water dose was not high enough in the previous study to saturate all the surface reactions i.e. only reaction 32, not reaction 33, was saturated in the previous study. With higher water doses the temperature did not have any major effect on the reaction mechanism. At low temperatures (150 - 250 ^{o}C) somewhat above 50 % and at high temperatures (300 - 400 ^{o}C) less than 50 % of the ligands were released during the $Al(CH_3)_3$ pulse, and the rest during the D_2O pulse.

6.5.2 $SrTiO_3$ ALD Process

Due to the complicated nature of the ternary ALD oxide processes the $SrTiO_3$ process was studied first by monitoring the SrO process, then by studying how SrO grows on TiO_2 and finally the $SrTiO_3$ process itself. The strontium precursor in all these studies was strontium bis(tri-isopropylcyclopentadienyl) [$Sr(C_5{}^{i}Pr_3H_2)_2$]. The oxygen and titanium sources were deuterated water and titanium isopropoxide. Most of the studies were carried out at 325 ^{o}C because at that temperature the films were already crystalline and the best electrical properties were obtained.[136,137] However, recent results[VII,138] suggest that a ALD reaction temperature of 325 ^{o}C is already too high for both metal precursors and therefore lower temperatures should be used. Due to these reasons, some unpublished data measured at 250 ^{o}C will also be presented here.

SrO at 250 ^{o}C. At 250 ^{o}C the same growth rate was observed with both 5 and 7 s strontium precursor pulse lengths i.e. the strontium precursor was not decomposing. According to QCM data 70 % of the ligands were already released during the strontium precursor pulse. According to this result a simplified reaction can be suggested:

$$3\text{-}OD(s) + 2\ Sr({}^{i}Pr_3Cp)_2(g) \rightarrow O\text{-}Sr\text{-}O(s) + \text{-}O\text{-}Sr\ {}^{i}Pr_3Cp\ (s) + 3D{}^{i}Pr_3Cp\ (g) \qquad (34)$$

In this reaction one ligand per two strontium ions is left on the surface. The tri-isopropylcyclopentadienyl ($^{i}Pr_3Cp$) ligands are relatively large and therefore it can be suggested that the surface after the strontium precursor pulse has two kinds of strontium species. One is bonded only to surface oxygen and the other to both surface oxygen and one $^{i}Pr_3cp$ ligand. This means that one ligand per two strontium ions would be left on the surface after the strontium precursor pulse (Fig. 17).

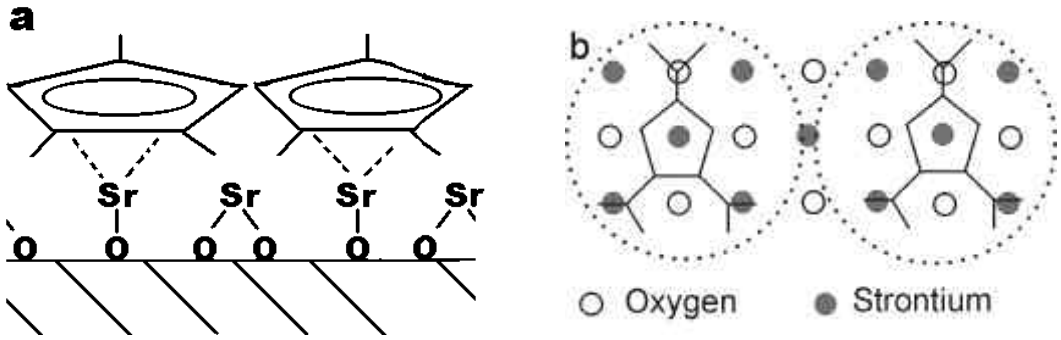

Figure 17. Proposed SrO surface after strontium precursor pulse. a) a side view and b) a top view along (100) plane. The dashed circle presents the estimated sterical hindrance caused by the tri-isopropylcyclopentadienyl ligand.

The main orientation of the ALD grown SrO layer is (111) and (100).[139] Figure 17 b shows a top view along (100) plane. The distance between two strontium ions along the [100] axis is 5.2 Å.[255] The diameter of the cross section of tri-isopropylcyclopentadienyl ligand estimated from the crystal structure of $Sr(^{i}Pr_3Cp)_2$ [256] is 11.5 Å, which is in relatively good agreement with the distance between two strontium. This is a good example why the growth rate is less than a full monolayer per cycle. However, the calculations proposed above are relatively crude and more sophisticated computer based models should be used to obtain more accurate results.

During the water pulse the rest of the ligands are released:

$$(\text{-O-})_2\text{Sr(s)} + \text{-OSr}\,^{i}\text{Pr}_3\text{cp(s)} + 2\text{D}_2\text{O(g)} \rightarrow \text{2-O-Sr-OD(s)} + \text{-OD(s)} + \text{D}\,^{i}\text{Pr}_3\text{cp (g)} \qquad (35)$$

Figure 18. shows a schematic presentation of the surface before and after the water pulse.

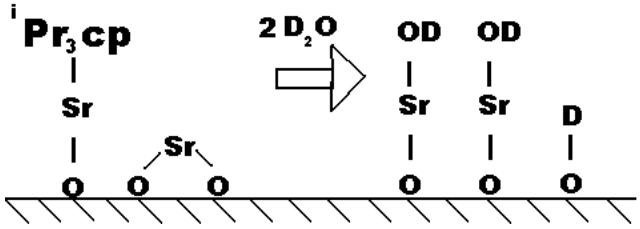

Figure 18. The proposed SrO surface before and after the water (D_2O) pulse.

Water is very reactive towards cyclopentadienyl ligand and, on the other hand, the strontium oxide hydrolyzes relatively easily and therefore it can be proposed that both surface species are converted to hydroxyl groups. If this is the case, the surface would be the same as in the beginning of the ALD cycle and therefore ready to receive the next ALD cycle.

SrO at 325 °C. The growth rate determined with QCM did not saturate as a function of water pulse.[X] It is possible that the water dose was not large enough. However, the water dose used (5 s) exceeded the doses usually needed for oxide growth in the same reactor[V-VIII] and therefore longer D_2O pulses were not used. Strontium oxides are known to form hydroxides very easily and therefore it was suggested that with long water pulses the strontium oxide would start to form strontium hydroxides:[137]

$$SrO(s) + H_2O(g) \rightarrow Sr(OH)_2(s) \quad (36)$$

The growth rate did not saturate as a function of strontium precursor pulse either. This was proposed to be due to the thermal decomposition of the strontium precursor at 325 °C. The growth rate versus strontium precursor pulse curve showed two separate steps (see ref. **X** Fig.2 b). In the first stage the growth rate increased relatively quickly and saturated to an almost constant level. When the pulse length was over 5 s the growth rate increased rapidly. This suggests that the thermal decomposition process is essentially slower than the ALD type exchange reactions. This is the reason why the thermal decomposition was not extensive in the ALD reactor with small substrates where only short precursor pulse lengths were needed.[136,137] In a reactor with larger substrates and longer heated source lines the decomposition was clearly observed.[138]

SrO on TiO_2 at 250 °C. At 250 °C the TiO_2 surface had no effect on the growth rate of SrO (Fig. 19 a). In addition, the SrO growth rate was also independent of the amount of TiO_2 deposited beforehand. These results suggest that the film grows more like a solid mixture of two oxides than $SrTiO_3$ phase. This is in accordance with film growth studies[136,137] where at 250 °C the films were usually amorphous and only with well crystalline substrates, such as platinum or $SrTiO_3$ single crystal, some crystallinity was obtained.[139]

SrO on TiO_2 at 325 °C. When SrO was grown on TiO_2 at 325 °C the growth rate was always higher during the first cycles than during the period of constant growth (Fig. 19 b). In addition, the growth rate stayed at a constant level when SrO was grown on SrO after a break (90 s), and therefore surface reconstruction and other possible slow processes which could change the growth can be ruled out. In addition, during the first cycles over 90 % of the ligands were already removed during the strontium pulse. These facts suggest that the TiO_2 surface promotes SrO incorporation due to formation of the thermodynamically favorable $SrTiO_3$. The same effect was observed also when TiO_2 was grown on SrO but to a lesser extent. It was calculated that it takes about six cycles to grow a full monolayer of TiO_2. It was interesting that according to both QMS and QCM data it took about five cycles to obtain the constant growth rate. In addition, it was noticed that the growth rate was lower when the starting layer was only a fraction of a monolayer of TiO_2 (two cycles of TiO_2) than when the film surface was fully covered with TiO_2 (ten cycles of TiO_2). This is understandable because if there is a full monolayer of TiO_2 more $SrTiO_3$ can form.

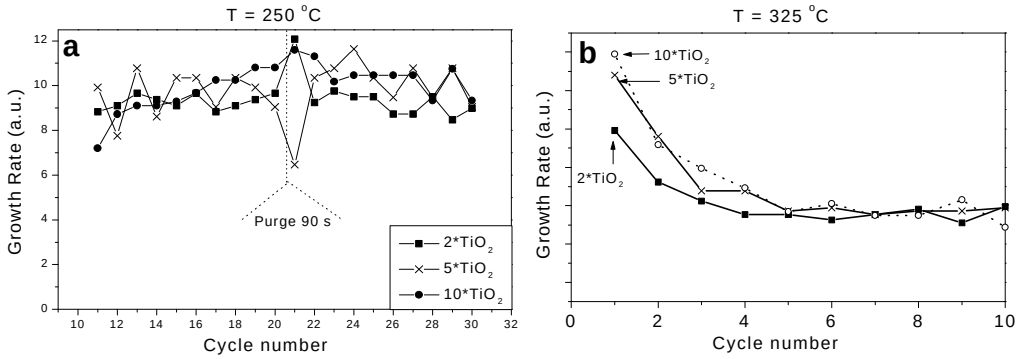

Figure 19. The growth rate of SrO as a function of cycle number at a) 250 °C b) 325 °C. In a) first ten cycles of SrO were grown and after that 2, 5, or 10 cycles of TiO_2 (not shown). Then again ten cycles of SrO and after a 90 second pause again ten cycles of SrO. In b) ten cycles of SrO were grown on the surface where 2, 5, or 10 cycles of TiO_2 had been deposited beforehand. [X]

$SrTiO_3$ at 250 °C. The pulsing order consisted of first one cycle SrO and then one cycle TiO_2. The growth rate of both SrO and TiO_2 was already constant from the second pulse as measured with QCM. The ratio between the growth rates, i.e. m_0 (SrO) and $m_0(TiO_2)$ was about 0.8, which is somewhat lower than the calculated value of 1.3 for stoichiometric $SrTiO_3$. Most of the Cp ligands i.e. 70 - 80 % were already released during the strontium precursor pulse as calculated from the QMS and QCM data. On the other hand, 60 - 70 % of the isopropoxide ligands were released during the titanium precursor pulse as measured with QCM and QMS. Both results are close to the binary growth studies where at 250 °C in the SrO[X] and TiO_2 processes[VII] 70 % and 50 % of the ligands were released during the metal precursor pulses. The $SrTiO_3$ growth at 250 °C was well behaved and no effect from the growth surface was observed. This result is in accordance with the results from the binary growth studies at 250 °C presented above.

$SrTiO_3$ at 325 °C. As already discussed, the reaction temperature of 325 °C is relatively high for the metal precursors used. This causes that the signal in the data (ref. X, Fig. 5) does not stay at constant level. However, some results can be obtained from these measurements.

The pulsing order consisted of first one cycle of SrO and then one cycle of TiO_2. The growth rate of SrO decreased during the first four pulses but after it that saturated to a constant level. The ratio between the constant growth rates, i.e. m_0, during the SrO and TiO_2 cycles was:

$$\frac{m_0(SrO)}{m_0(TiO_2)} = \frac{3.7Hz}{2.7Hz} = 1.4 \qquad (37)$$

For a stoichiometric $SrTiO_3$, the ratio between the mass increments during the SrO and TiO_2 cycles should be:

$$\frac{M(SrO)}{M(TiO_2)} = \frac{103.6}{79.9} = 1.30 \qquad (38)$$

The experimental and calculated results are in relatively good agreement with each other. However, it should be noted that at 325 ^{o}C the metal ratio does not necessarily settle to unity, but depends on the strontium precursor pulse length and the SrO to TiO_2 cycle ratio.[136,137] Therefore, the *in situ* studies are a promising method for adjusting the metal ratio in the ternary processes. Simultaneously to the QCM studies the amount of reaction byproducts were monitored with QMS. When the m_0 to m_1 ratio was 1.4, 75 % of the cyclopentadienyl ligands were released during the strontium precursor pulse and the rest during the water pulse.

7. Conclusions and Remarks

The thesis concentrated on the growth and *in situ* studies on ALD oxides relevant to microelectronic devices. $Zr_xTi_yO_z$ thin films were grown using a novel metal halide-metal alkoxide approach. The idea was to avoid the need of a strong oxidizer during the process and thereby avoid the formation of interfacial SiO_2, which would negate the benefits of high permittivity oxides. $Zr_xTi_yO_z$ thin films deposited by this method had a permittivity of 45 - 65 and leakage current of 10^{-4} A/cm^2 at 0.2 MV/cm. The interfacial layer formation was not studied in the $Zr_xTi_yO_z$ process but it was possible to deposit Al_2O_3 on silicon without a SiO_2 interfacial layer. In the $ZrCl_4$ - $Ti(OCH(CH_3)_2)_4$ process two parallel reaction paths were found. The major part of the reactions were occurring through the release of $(CH_3)_2CHCl$ while the minor part (20 %) of the reactions were occurring through HCl and CH_2CHCH_3 release.

The reaction mechanisms were studied by using a novel QMS - QCM setup. The main disadvantage of the QCM method is the temperature sensitivity and therefore methods for compensating the temperature effect were described. Because ALD reactions are self-limiting the composition of binary films is usually relatively easy to control. However, in ternary or more complicated processes the exact stoichiometry is hard to obtain and the combination of all experimental variables is impossible to examine. *In situ* methods showed the possibility of monitoring the metal ratio of the growing film and therefore could assist in developing complicated processes.

The main drawback of the *in situ* system used in this study was that due to rapid ALD reactions it was impossible to scan all *m/z* values and therefore it was possible that some reaction byproducts were not found. One solution could be that reaction byproducts could be trapped and analyzed *ex situ*. Using this procedure the analysis time would be irrelevant. In addition, methods which need relative large sample size could be used. The main drawback would be the possible side reactions which could affect the results.

In the $ZrCl_4$ - D_2O process the growth rate was the highest at 300 ^oC. At lower temperatures the growth rate was lower due to kinetic reasons and at high temperatures due to lowered amount of hydroxyl groups at the surface. The decrease in the amount of hydroxyl groups as a function of temperature was also affecting the growth mechanism. At 250 ^oC half of the chlorides were released during the $ZrCl_4$ pulse while at higher temperatures the reaction mechanism was slowly changing to a direction where the incoming metal precursor reacted with only one hydroxyl group.

The onset temperature for the thermal decomposition of titanium alkoxides increased in the order of $Ti(OCH(CH_3)_2)_4$ (225 ^oC), $Ti(OC(CH_3)_3)_4$ (250 ^oC), $Ti(OC_2H_5)_4$ (300 ^oC) and $Ti(OCH_3)_4$ (350 ^oC). In the $Ti(OC_2H_5)_4$ - D_2O ALD process over 90 % of the reaction byproducts were released during the water pulse and the rest during the metal precursor pulse. Ethanol was observed to adsorb on TiO_2 surface. The ethanol readsorption was thus suggested to be the reason behind the small amount of reaction byproduct observed during the metal precursor pulse. In the $Ti(OCH(CH_3)_2)_4$ - D_2O process, below the decomposition temperature (225 ^oC), half of the reaction byproducts were released during the metal precursor pulse. Despite thermal decomposition the surface stayed isopropoxy terminated after the titanium isopropoxide pulse at least up to 350 ^oC.

In the $Al(CH_3)_3$ - D_2O process the highest growth rate was obtained at 250 ^oC. The dehydroxylation decreased the growth rate at higher temperatures. About half of the reaction byproducts were released during the metal precursor pulse and the rest during the water pulse. The temperature had no marked effect on the growth rate.

TiO_2 surface catalyzed the SrO growth at 325 ^oC, which was concluded to be due to the $SrTiO_3$ formation. On the other hand, at 250 ^oC this effect was not observed. Those results were in line with the previous film growth studies where at 250 ^oC the thin films were amorphous or weakly crystalline while at 325 ^oC they possessed more crystallinity. Most of the reaction byproducts were already released during the strontium precursor pulse. It was suggested that the maximum density of ligands on SrO surface could be one ligand per two adsorbed strontium atoms. This assumption was in line with the experimental results.

Several precursors were examined and the results were found to be in accordance with earlier film growth and *in situ* studies. This encourages us to believe that the system works with different kinds of processes. At the moment all processes studied were already known to work and therefore in the future it would be interesting to study completely unknown processes and see how well those results would guide the thin film growth experiments. In addition, there are still a lot of known ALD processes which need to be studied, such as metal nitride, and sulfide ALD processes.

The combination of modeling and *in situ* studies would be interesting. With modeling it would be possible to estimate which reactions are energetically feasible and which are not. Those theories could be tested with the *in situ* experiments. It is supposed that by following this path new processes would be much faster to develop.

Acknowledgements

The thesis is based on experimental work carried out during the years 1999 - 2002 in the laboratory of inorganic chemistry at the university of Helsinki.

I am grateful to my supervisors Doc. Mikko Ritala and Prof. Markku Leskelä for their excellent guidance thought my journey towards PhD.

Ms. Eija Koskenlinna and Ms. Saara Abdalla are thanked for revising the English language of this thesis. Special thanks for the co-authors Ms. Raija Matero, Dr. Marika Juppo, Dr. Kaupo Kukli, Mr. Teemu Alaranta and Mr. Timo Hänninen. Mr. Timo Sajavaara and Prof. Juhani Keinonen are acknowledged for the TOF-ERDA analysis of the thin films.

I would like to thank Antti, Marko, Petri, Marianna, Heini, Timo, O -fail and all of my dearest friends and colleagues at the laboratory of inorganic chemistry for the nice working atmosphere. In addition, I wish to thank Mr. Jarkko Ihanus for sharing the same office and many interesting discussions. I would like to thank Anu, Jerker, Kati, Petteri, Lauri, Mikko, Santtu, Merle, Wee and the people of Kek society, just to mention some, and all my friends for the happy moments we have had.

I would like to thank for the support and good advice from my father Ilkka and my mother Sirpa, even that you, Sirpa, didn't understand a thing what I was doing :-)

The Academy of Finland, the National Technology Agency (TEKES), Finnish Chemists Society, the Finnish Cultural Foundation and Technical Development Foundation are acknowledged for the financial support.

Helsinki, August 2002

Antti Rahtu

References

I M. Ritala, K. Kukli, A. Rahtu, P. I. Räisänen, M. Leskelä, T. Sajavaara, J. Keinonen, *Science*, 288 (**2000**) 319 - 321.
II A. Rahtu, M. Ritala, M. Leskelä, *Chem. Mater.*, 13 (**2001**) 1528 - 1532.
III A. Rahtu, M. Ritala, *Electrochem. Soc. Proc.*, 2000-13 (**2000**)105 - 111.
IV A. Rahtu, M. Ritala, *Appl. Phys. Lett.*, 80 (**2002**) 521- 523.
V A. Rahtu, T. Alaranta, M. Ritala, *Langmuir*, 17 (**2001**) 6506- 6509.
VI A. Rahtu, K. Kukli, M. Ritala, *Chem. Mater.*, 13 (**2001**) 817- 823.
VII A. Rahtu, M. Ritala, *Chem. Vap. Deposition.* 8 (**2002**) 21- 28.
VIII A. Rahtu, M. Ritala, *J. Mater. Chem.*, 12 (**2002**) 1484-1489.
IX A. Rahtu, M. Ritala, Manuscript.
X A. Rahtu, T. Hänninen, M. Ritala, *J. Phys. IV*, 11 (**2001**) Pr3-923 - 930.

---

[1] M. L. Green, E. P. Gusev, R. Degraeve, E. L. Garfunkel, *J. Appl. Phys.*, 90 (**2001**) 2057 - 2121.
[2] G. D. Wilk, R.M. Wallace, J. M. Anthony, *J. Appl. Phys.*, 89 (**2001**) 5243 - 5275.
[3] M. A. Subramanian, R. D. Shannon, *Mater. Res. Bull.*, 24 (**1989**) 1477 - 1483.
[4] G. D. Wilk, R. M. Wallace, *Appl. Phys. Lett.*, 74 (**1999**) 2854 - 2856.
[5] L. Manchanda, M. L. Green, R. B. van Dover, M. D. Morris, A. Kerber, Y. Hu, J.- P. Han, P. J. Silverman, T. W. Sorsch, G. Weber, V. Donnelly, K. Pelhos, F. Klemens, N. A. Ciampa, A. Kornblit, Y. O. Kim, J. E. Bower, D. Barr, E. Ferry, D. Jacobson, J. Eng, B. Busch, H. Schulte., *Tech. Dig. Int. Electron Devices Meet.*, **2000**, 23-26.
[6] J. Y.-M. Lee, B. C. Lai, The electrical properties of high - dielectric constant and ferroelectric thin films for very large scale integration circuits in *Handbook of Thin Film Materials*, (Ed: H. S. Nalwa), Academic Press, San Diego **2001**, Vol. 3. Ch. 1.
[7] C. S. Hwang, *Mater. Sci. Eng.*, B56 (**1998**) 178 - 190.
[8] A. I. Kingon, S. K. Streiffer, C. Basceri, S. R. Summerfelt, *MRS Bull.*, 21 (**1996**) 46 - 52.
[9] D. Kahn, M. M. Atalla, IRE Solid State Device Res. Conf., Pittsburgh, P.A., **1960**.
[10] G. E. Moore, *Electronics*, 38 (**1965**).
http://www.intel.com/research/silicon/mooreslaw.htm
[11] J. Robertson, *J. Vac. Sci. Technol.*, B 18 (**2000**)1785 - 1791.
[12] M. Copel, M. Gribelyuk, E. Gusev, *Appl. Phys. Lett.*, 76 (**2000**) 436 - 438.
[13] A. I. Kingon, J.-P. Maria, S. K. Streiffer, *Nature*, 406 (**2000**) 1032 - 1038.
[14] C. Zhao, G. Roebben, H. Bender, E. Young, S. Haukka, M. Houssa, M. Naili, S. De Gendt, M. Hayns, O. Van Der Biest, *Microelectron. Reliab.*, 41 (**2001**) 995 - 998.
[15] T. Suntola, J. Antson, **1977**, US Patent No. 4 058 430.
[16] M. Ritala, M. Leskelä, Atomic Layer Deposition in *Handbook of Thin Film Materials*, (Ed: H. S. Nalwa), Academic Press, San Diego **2002**, Vol. 1., 103 - 159.
[17] M. Ritala, *Ann. Acad. Sci. Fenn.*, Ser. A, 257 (**1994**).
[18] K. Kukli, *Dissert. Phys. Univ. Tartuensis*, 27 (**1999**).
[19] T. Suntola, J. Antson, A. Pakkala, S. Lindfors, *SID 80 Digest* 11(**1980**) 108 -109.
[20] T. Suntola, *Mater. Sci. Rep.* 4(**1989**) 261 - 312.

[21] T. Suntola, Atomic Layer Epitaxy in *Handbook of Crystal Growth 3*, Thin Films and Epitaxy, Part B: Growth Mechanisms and Dynamics, Elsevier, 1994; Chapter 14.
[22] L. Niinistö, M. Ritala, M. Leskelä, *Mater. Sci. Eng.*, B41(**1996**) 23 - 29.
[23] M. Leskelä, M. Ritala, *J. Phys. IV*, C-5 (**1995**) 937 - 951.
[24] M. Ritala, M. Leskelä, J.- P. Dekker, C. Mutsaers, P. J. Soininen, J. Skarp, *Chem. Vap. Deposition*, 5 (**1999**) 7 - 9.
[25] M. Ritala, *Appl. Surf. Sci.*, 112 (**1997**) 223 - 230.
[26] J. W. Klaus, O. Sneh, S. M. George, *Science*, 278 (**1997**) 1934 - 1936.
[27] J. W. Klaus, A. W. Ott, J. M. Johnson, S. M. George, *Appl. Phys. Lett.*, 70 (**1997**)1092-1094.
[28] J. W. Klaus, O. Sneh, A. W. Ott, S. M. George, *Surf. Rew. Lett.*, 6 (**1999**) 435-448.
[29] M. Ritala, private communication.
[30] N. H. Karam, H. Liu, I. Yoshida, S. M. Bedair, *Appl. Phys. Lett.*, 52 (**1988**) 1144 - 1146.
[31] S. M. Rossnagel, A. Sherman, F. Turner, *J. Vac. Sci. Technol.*, B18 (**2000**) 2016 - 2020.
[32] H. Goto, K. Shibahara, S. Yokoyama, *Appl. Phys. Lett.*, 68 (**1996**) 3257 - 3259.
[33] C.-W. Jeong, J.-S. Lee, S.-K. Joo, *Jpn. J. Appl. Phys.*, 40 (**2001**) 285-289.
[34]H.-J. Song, C.-S. Lee, S.-W. Kang, *Electrochem. and Solid State Lett.*, 4 (**2001**) F13-F14.
[35] J.-S. Park, H.-S. Park, S.-W. Kang, *J. Electrochem. Soc.*, 149 (**2002**) C28 - 32.
[36] H. Kim, S. M. Rossnagel, *J. Vac. Sci. Technol.*, A20 (**2002**) 802-808.
[37] M. Leskelä, M. Ritala, *Thin Solid Films*, 409 (**2002**) 138 - 146.
[38] D. Ha, D. Shin, G.-H. Koh, J. Lee, S. Lee, Y.-S. Ahn, H. Jeong, T. Chung, K. Kim, *IEEE Trans. Electr. Dev.*, 47 (**2000**) 1499- 1506.
[39] http://www.intel.com/research/silicon/
[40] M. Leskelä, W.-M. Li, M. Ritala, Materials in Thin Film Electroluminescent Devices, *Semiconductors and Semimetals, 65 (Electroluminescence II)*, Ed G. O. Mueller, Academic Press, San Diego **2000**, p. 107 -182.
[41]A. Kytökivi, E. - L. Lakomaa, A. Root, H. Österholm, J. - P. Jacobs, H. Brongersma, *Langmuir*, 13 (**1997**) 2717 - 2725.
[42] S. Haukka, E.-L. Lakomaa, T. Suntola, *Stud. Surf. Sci. Catal.*, 120 (**1998**) 715 - 750.
[43] T. I. Hukka, T. A. Pakkanen, M. P. D'Evelyn, *J. Phys. Chem.*, 99 (**1995**) 4710-4719.
[44] P. Mårtensson, K. Larsson, J.-O. Carlsson, *Appl. Surf. Sci.*, 148 (**1999**) 9-16.
[45] H.-S. Park, J.-S. Min, J.-W. Lim, S.-W. Kang, *Appl. Surf. Sci.*, 158 (**2000**) 81-91.
[46] Y. Widjaja, C. B. Musgrave, *Appl. Phys. Lett.*, 81 (**2002)** 304-306.
[47] V. V. Brodskii, E. A. Rykova, A. A. Bagatur'yants, A. A. Korkin, *Com. Mater. Sci.*, 24 (**2002**) 278 - 283.
[48] A. R. Barron, In *CVD of nonmetals*; Ed. W. S. Jr. Rees, VCH: Weinheim, **1996**, p. 282.
[49] E. P. Gusev, M. Copel, E. Cartier, I. J. R. Baumvol, C. Krug, M. A. Gribelyuk, *Appl. Phys. Lett.*, 76 (**2000**) 176 - 178.
[50] E. P.Gusev, M. Copel, E. Cartier, D.Buchanan, H. Okorn-Schmidt, M. Gribelyuk, D. Falcon, R. Murphy, S. Molis, I. J. R. Baumvol, C. Krug, M. Jussila, M. Tuominen, S. Haukka, *Electrochem. Soc. Proc.*, 2 (**2000**) 477 - 485.
[51] Y.-C. Jung, H. Miura, M. Ishida, *Jpn. J. Appl. Phys.*, 38 (**1999**) 2333 - 2336.

[52] K. J. Hubbard, D. G. Schlom, *J. Mater. Res.*, 11(**1996**) 2757 - 2776.
[53] P. I. Räisänen, M. Ritala, M. Leskelä, *J. Mater. Chem.*, 12 (**2002**) 1415-1418.
[54] J. Wang, Y.-H. Yu, S. C. Lee, Y.-W. Chung, *Surf. Coat. Tech.*, 146-147 (**2001**) 189-194.
[55] N. Bahlawane, T. Watanabe, *J. Am. Ceram. Soc.*, 83 (**2000**) 2324-2326.
[56] R. J. P. Corriu, D. Leclercq, *Angew. Chem. Int. Ed. Engl.*, 35 (**1996**) 1420-1436.
[57] M. Aguilar-Frutis, M. Garcia, C. Falcony, *Appl. Phys. Lett.*, 72 (**1998**) 1700-1702.
[58] M. Aguilar-Frutis, M. Garcia, C. Falcony, G. Plesch, S. Jimenez-Sandoval, *Thin Solid Films*, 389 (**2001**) 200 - 206.
[59] J. Guzmán-Mendoza, M. García-Hipólito, M. Aguilar-Frutis, C. Falcony-Guajardo, *J. Phys. Condens. Matter.*, 13 (**2001**) L955-L959.
[60] B. Hirschauer, S. Söderholm, G. Chiaia, U. O. Karlsson, *Thin Solid Films*, 305 (**1997**) 243 - 247.
[61] S. W. Whangbo, Y. K. Choi, H. K. Jang, Y. D. Chung, I. W. Lyo, C. N. Whang, *Thin Solid Films*, 388 (**2001**) 290 - 294.
[62] S. Ruppi, A. Larsson, *Thin Solid Films*, 388 (**2001**) 50 - 61.
[63] T. Maruyama, S. Arai, *Appl. Phys. Lett.*, 60 (**1992**) 322- 323.
[64] T. Maruyama, T. Nakai, *Appl. Phys. Lett.*, 58 (**1991**) 2079- 2080.
[65] E. Fredriksson, J.-O. Carlsson, *J. Chem. Vap. Deposition*, 1 (**1993**) 333 - 417.
[66] W. Koh, S.-J. Ku, Y. Kim, *Thin Solid Films*, 304 (**1997**) 222-224.
[67] L. Hiltunen, H. Kattelus, M. Leskelä, M. Mäkelä, L. Niinistö, E. Nykänen, P. Soininen, M. Tiitta, *Mater. Chem. Phys.*, 28 (**1991**) 379 - 388.
[68] G. Oya, M. Yoshida, Y. Sawada, *Appl. Phys. Lett.*, 51 (**1987**) 1143 - 1145.
[69] K. Kukli, M. Ritala, M. Leskelä, J. Jokinen, *J. Vac. Sci. Technol.*, A15 (**1997**) 2214-2218.
[70] A. W. Ott, K. C. McCarley, J. W. Klaus, J. D. Way, S. M.George, *Appl. Surf. Sci.* 107 (**1996**)128 -136.
[71] E.-L. Lakomaa, A. Root, T. Suntola, *Appl. Surf. Sci.*, 107(**1996**) 107 - 115.
[72] H. Kumagai, K. Toyoda, M. Matsumoto, M. Obara, *Jpn. J. Appl. Phys.*, 32 (**1993**) 6137-6140.
[73] G. S. Higashi, C. G. Fleming, *Appl. Phys. Lett.*, 55 (**1989**) 1963-1965.
[74] A. W. Ott, J. W. Klaus, J. M. Johnson, S. M .George, *Thin Solid Films*, 292 (**1997**) 135-144.
[75] B. O'Regan, M. Grätzel, *Nature*, 353 (**1991**) 737 - 739.
[76] A. Hagfeldt, M. Grätzel, *Chem. Rev.*, 95 (**1995**) 49 - 68.
[77] M .A. Fox, M. T. Dulay, *Chem. Rev.*, 93 (**1993**) 341 - 357.
[78] M. R. Hoffmann, S. T. Martin, W. Choi, D. W. Bahnemann, *Chem. Rev.*, 95 (**1995**) 69 - 96.
[79] A. Fujishima, T. N. Rao, D. A. Tryk, *Electrochim. Acta*, 45 (**2000**) 4683-4690.
[80] G. P. Burns, I. S. Baldwin, M. P. Hastings, J. G. Wilkes, *J. Appl. Phys.*, 66 (**1989**) 2320 - 2324.
[81] M. Gómez, J. Rodríguez, S. Tingry, A. Hagfeldt, S.-E. Lindquist, C. G. Granqvist, *Sol. Energ. Mat. Sol. C.*, 59 (**1999**) 277-287.
[82] E. Sánchez, T. López, R. Gómez, Bokhimi, A. Morales, O. Novaro, *J. Solid. State Chem.*, 122 (**1996**) 309-314.
[83] N. Kaliwoh, J.-Y. Zhang, I. W. Boyd, *Surf. Coat. Technol.*, 125 (**2000**) 424-427.

[84] M. L. Hitchman, S. E. Alexandrov, *Electrochem. Soc. Interface*, 10 (**2001**) 40-45.
[85] S. A. Campbell, D. C. Gilmer, X. Wang, M. Hsieh, H.-S. Kim, W. L. Gladfelter, J. Yan, *IEEE Trans. Electr. Dev.*, 44 (**1997**) 104 - 109.
[86] Y. Takahashi, H. Suzuki, M. Nasu, *J. Chem. Soc. Faraday Trans.*, 81 (**1985**) 3117-3125.
[87] Y. Takahashi, K. Tsuda, K. Sugiyama, H. Minoura, D. Makino, M. Tsuiki, *J. Chem. Soc. Faraday Trans.*, 77 (**1981**) 1051-1057.
[88] G. A. Battiston, R. Gerbasi, A. Gregori, M. Porchia, S. Cattarin, G. A. Rizzi, *Thin Solid Films*, 371 (**2000**) 126-131.
[89] M. Ritala, M. Leskelä, E. Nykänen, P. Soininen, L. Niinistö, *Thin Solid Films*, 225 (**1993**) 288 - 295.
[90] J. Aarik, A. Aidla, A. -A. Kiisler, T. Uustare, V. Sammelselg, *Thin Solid Films*, 305 (**1997**) 270 - 273.
[91] J. Aarik, A. Aidla, H. Mändar, T. Uustare, *Appl. Surf. Sci.*, 172 (**2001**)148-158.
[92] J. Aarik, A. Aidla, H. Mändar, V. Sammelselg, *J. Cryst. Growth*, 220 (**2000**) 531-537.
[93]J. Aarik, A. Aidla, V. Sammelselg, H. Siimon, T. Uustare, *J. Cryst. Growth*, 169 (**1996**) 496-502.
[94] J. Aarik, A. Aidla, T. Uustare, V. Sammelselg, *J. Cryst. Growth*, 148 (**1995**) 268-275.
[95] A. Niilisk, A. Rosental, A. Gerst, V. Sammelselg, T. Uustare, *Proc. SPIE*, 4318 (**2001**) 72-77.
[96] K. Kukli, M. Ritala, M. Schuisky, M. Leskelä, T. Sajavaara, J. Keinonen, T. Uustare, A. Hårsta, *Chem. Vap. Deposition*, 6 (**2000**) 303 - 310.
[97] K. Kukli, A. Aidla, J. Aarik, M. Schuisky, A. Hårsta, M. Ritala, M. Leskelä, *Langmuir*, 16 (**2000**) 8122 - 8128.
[98] M. Schuisky, A. Hårsta, A. Aidla, K. Kukli, A.-A. Kiisler, J. Aarik, *J. Electrochem. Soc.*, 147 (**2000**) 3319 - 3325.
[99] M. Schuisky, J. Aarik, K. Kukli, A. Aidla, A. Hårsta, *Langmuir*, 17 (**2001**) 5508-5512.
[100] M. Ritala, M. Leskelä, E. Rauhala, *Chem. Mater.*, 6 (**1994**) 556 - 561.
[101] J. Aarik, A. Aidla, V. Sammelselg, T. Uustare, M. Ritala, M.Leskelä, *Thin Solid Film*, 370 (**2000**) 163 - 172.
[102] M. Ritala, M. Leskelä, L. Niinistö, P. Haussalo, *Chem. Mater.*, 5 (**1993**) 1174 - 1181.
[103] J. Aarik, A. Aidla, T. Uustare, M. Ritala, M. Leskelä, *Appl. Surf. Sci.*,161 (**2000**) 385 - 395.
[104] H. O. Pierson, *Handbook of Chemical Vapor Deposition: Principles, Technology and Applications*, Noyes Publications, New Jersey **1992**.
[105] H. Kattelus, M.Ylilammi, J. Salmi, T. Ranta-aho, E. Nykänen, I. Suni, *Mater. Res. Soc. Symp. Proc.*, 284 (**1993**) 511 - 516.
[106] J. Shappir, A. Anis, I. Pinsky, *IEEE Trans. Electron. Dev.*, ED-33 (**1986**) 442 - 449.
[107] M. Morita, H. Fukumoto, T. Imura, Y. Osaka, M. Ichihara, *J. Appl. Phys.*, 58 (**1985**) 2407 - 2409.
[108] T. Ngai, W. J. Qi, R. Sharma, J. Fretwell, X. Chen, J. C. Lee, S. Banerjee, *Appl. Phys. Lett.*, 76 (**2000**) 502 - 504.
[109] A. Mehner, H. Klümper-Westkamp, F. Hoffmann, P. Mayr, *Thin Solid Films*, 308-309 (**1997**) 363-368.
[110] J. J. Yu, J.-Y. Zhang, I. W. Boyd, *Appl. Surf. Sci.*, 186 (**2002**) 190-194.
[111] M. A. Cameron, S. M. George, *Thin Solid Films*, 348 (**1999**) 90-98.

[112] J.S.Na, D.-H. Kim, K. Yong, S.-W. Rhee, *J. Electrochem. Soc.*, 149 (**2002**) C23 - 27.
[113] B. J. Gould, I. M. Povey, M. E. Pemble, W. R. Flavell, *J. Mater. Chem.*, 4 (**1994**) 1815-1819.
[114] T. Belmonte, T. Czerwiec, J. Gavillet, H. Michel, *Surf. Coat. Technol.*, 97 (**1997**) 642-648.
[115] M. Houssa, M. Tuominen, M. Naili, V. Afanas'ev, A. Stesmans, S. Haukka, M. M. Heyns, *J. Appl. Phys.*, 87 (**2000**) 8615 - 8620.
[116] S. Haukka, M. Tuominen, E. Granneman, *Semicon Europa 2000 / Semieducation*, 4. - 6. April **2000**, Munich, Germany.
[117] M. Ritala and M. Leskelä, *Appl. Surf. Sci.*, 75 (**1994**) 333 - 340.
[118] J. Aarik, A. Aidla, H. Mändar, T. Uustare, V. Sammelselg, *Thin Solid Films*, in press.
[119] K. Kukli, K. Forsgren, M. Ritala, M. Leskelä, J. Aarik, A. Hårsta, *J. Electrochem. Soc.*, 148 (**2001**) F227-F232.
[120] K. Kukli, K. Forsgren, J. Aarik, T. Uustare, A. Aidla, A. Niskanen, M. Ritala, M. Leskelä, A. Hårsta, *J. Cryst. Growth*, 231 (**2001**) 262 - 272.
[121] K. Kukli, M. Ritala, M. Leskelä, *Chem. Vap. Deposition*, 6 (**2000**) 297 - 302.
[122] R. Matero, M. Ritala, M. Leskelä, A. C. Jones, P. A. Williams, J. F. Bickley, A. Steiner, T. J. Leedham, H. O. Davies, *J. Non-cryst. Solids*, 303 (**2002**) 24-28.
[123] K. Eisenbeiser, J. M. Finder, Z. Yu, J. Ramdani, J. A. Curless, J. A. Hallmark, R. Droopad, W. J. Ooms, L. Salem, S. Bradshaw, C. D. Overgaard, *Appl. Phys. Lett.*, 76 (**2000**) 1324 - 1326.
[124] R. A. McKee, F. J. Walker, M. F. Chrisholm, *Phys. Rew. Lett.*, 81 (**1998**) 3014 - 3017.
[125] Y. Fukuda, K. Aoki, K. Numata, A. Nishimura, *Jpn. J. Appl. Phys.*, 33 (**1994**) 5255-5258.
[126] S. H. Nam, N. H. Cho, H. G. Kim, *J. Phys. D: Appl. Phys.*, 25 (**1992**) 727-729.
[127] B. K. Moon, H. Ishiwara, *Jpn. J. Appl. Phys.*, 33 (**1994**) 1472 - 1477.
[128] M. B. Lee, H. Koinuma, *J. Appl. Phys.*, 81 (**1997**) 2358 - 2362.
[129] P. C. Joshi, S. B. Krupanidhi, *J. Appl. Phys.*, 73 (**1993**) 7627 - 7634.
[130] G. W. Dietz, W. Antpöhler, M. Klee, R. Waser, *J. Appl. Phys.*, 78 (**1995**) 6113 - 6121.
[131] C. S. Kang, C. S. Hwang, H.-J. Cho, B. T. Lee, S. O. Park, J. W. Kim, H. Horii, S. I. Lee, Y. B. Koh, M. Y. Lee, *Jpn. J. Appl. Phys.*, 35 (**1996**) 4890-4895.
[132] T. Kimura, H. Yamauchi, H. Machida, H. Kokubun, M. Yamada, *Jpn. J. Appl. Phys.*, 33 (**1994**) 5119-5124.
[133] S. Momose, T. Nakamura, K. Tachibana, *Jpn. J. Appl. Phys.*, 39 (**2000**) 5384-5388.
[134] Y. B. Hahn, D. O. Kim, *J. Vac. Sci. Technol.*, A17 (**1999**) 1982-1986.
[135] A. Kosola, M. Putkonen, L. Niinistö, CERC3 Young Chemists Workshop, Tuusula, Finland, May 20-23. 1999.
[136] M. Vehkamäki, T. Hatanpää, T. Hänninen, M. Ritala, M. Leskelä, *Electrochem. Solid State Lett.*, 2 (**1999**) 504 - 506.
[137] M. Vehkamäki, T. Hänninen, M. Ritala, M. Leskelä, T. Sajavaara, E. Rauhala, J. Keinonen, *Chem. Vap. Deposition*, 7 (**2001**) 75 - 80.
[138] M. Vehkamäki, M. Linnermo, S. Haukka, M. Ritala, M. Leskelä, unpublished results.

[139] M. Vehkamäki, private communications.
[140] Joint Committee on Powder Diffraction Standards, Card 4-802, International Center for Diffraction Data, Newton Square, PA.
[141] Joint Committee on Powder Diffraction Standards, Card 35-734, International Center for Diffraction Data, Newton Square, PA.
[142] K. Kukli, M. Ritala, M. Leskelä, *Chem. Mater.*, 12 (**2000**) 1914 - 1920.
[143] E. S. Ramakrishnan, K. D. Cornett, G. H. Shapiro, W.-Y. Howng, *J. Electrochem. Soc.*, 145 (**1998**) 358 - 362.
[144] D.-A. Chang, P. Lin, T.-Y. Tseng, *J. Appl. Phys.* 78 (**1995**) 7103 - 7108.
[145] D.-A. Chang, P. Lin, T.-Y. Tseng, *J. Appl. Phys.*, 77 (**1995**) 4445 - 4451.
[146] D.-A. Chang, P. Lin, T.-Y. Tseng, *Appl. Phys. Lett.*, 64 (**1994**) 3252 - 3254.
[147] T. Kim, J. Oh, B. Park, K. S. Hong, *Appl. Phys. Lett.*, 76 (**2000**) 3043 - 3045.
[148] J. M. Miller, L. J. Lakshmi, *J. Phys. Chem. B*, 102 (**1998**) 6465 - 6470.
[149] R. Merkle, H. Bertagnolli, *J. Mater. Chem.*, 8 (**1998**) 2433 - 2439.
[150] O. Nakagawara, Y. Toyota, M. Kobayashi, Y. Yoshino, Y. Katayama, H. Tabata, T. Kawai, *J. Appl. Phys.*, 80 (**1996**) 388 - 392.
[151] Outokumpu HSC Chemistry for Windows program, Version 4.1, Outokumpu Research Oy, Pori, Finland, **1999.**
[152] L. W. Coughanour, R. S. Roth, V. A. DeProsse, *J. Res. Natl. Bur. Stand.*, 52 (**1954**) 37-42.
[153] Joint Committee on Powder Diffraction Standards, Card 34-0415, JCPDS, International Center for Diffraction Data, Newton Square, PA.
[154] K. Kukli, J. Aarik, A. Aidla, H. Siimon, M. Ritala, M. Leskelä, *Appl. Surf. Sci.*, 112 (**1997**) 236-242.
[155] K. Kukli, M. Ritala, M. Leskelä, *J. Electrochem. Soc.*, 142 (**1995**) 1670 - 1675.
[156] J. Aarik, K. Kukli, A. Aidla, L. Pung, *Appl. Surf. Sci.*, 103 (**1996**) 331 - 341.
[157] K. Kukli, J. Ihanus, M. Ritala, M. Leskelä, *Appl. Phys. Lett.*, 68 (**1996**) 3737 - 3739.
[158] K. Kukli, J. Ihanus, M. Ritala, M. Leskelä, *J. Electrochem. Soc.*, 144 (**1997**) 300 - 306.
[159] L. Bourget, R. J. P. Corriou, D. Leclercq, P. H. Mutin, A. Vioux, *J. Non-Cryst. Solids*, 242 (**1998**) 81 - 91.
[160] R. G. Gordon, J. Becker, D. Hausmann, S. Suh, AVS ALD meeting, 14-15 May, **2001**, Monterey, California, USA.
[161] E. Aro, S. Haukka, M. Tuominen, *International patent,* WO 01/40541 A1.
[162] R. G. Gordon, J. Becker, D. Hausmann, S. Suh, *Chem. Mater.*, 13 (**2001**) 2463-2464.
[163] J. Sterner, J. Kessler, L. Stolt, *J. Vac. Sci. Technol.*, A20 (**2002**) 278-284.
[164] J. W. Klaus, S. J. Ferro, S. M. George, *Thin Solid Films*, 360 (**2000**) 145-153.
[165] J. W. Klaus, S. J. Ferro, S. M. George, *J. Electrochem. Soc.*, 147 (**2000**) 1175 -1181.
[166] G. A. Battiston, R. Gerbasi, *Chem. Vap. Deposition*, 7 (**2001**) 225-229.
[167] S. M. George, O. Sneh, A. C. Dillon, M. L. Wise, A. W. Ott, L. A. Okada, J. D. Way, *Appl. Surf. Sci.*, 82/83 (**1994**) 460-467.
[168] A. W. Ott, J. W. Klaus, J. M. Johnson, S. M. George, K. C. McCarley, J. D. Way, *Chem. Mater.*, 9 (**1997**) 707-714.
[169] P. W. Jr. Morrison, O. Taweechokesupsin, *J. Electrochem. Soc.*, 145 (**1998**) 3212 - 3219.

[170] D. E. Aspnes, J. P. Harbison, A. A. Stunda, L. T. Florez, *Phys. Rev. Lett.*, 59 (**1987**) 1687 - 1690.
[171] A. Rosental, P. Adamson, A. Gerst, H. Koppel, A. Tarre, *Appl. Surf. Sci.*, 112 (**1997**) 82-86.
[172] A. Rosental, A. Tarre, P.Adamson, A. Gerst, A. Kasikov, A. Niilisk, *Appl. Surf. Sci.*, 142 (**1999**) 204-209.
[173] A. Tarre, A. Rosental, V. Sammelselg, T. Uustare, *Appl. Surf. Sci.*, 175-176 (**2001**) 111-116.
[174] A. I. Chowdhury, W. W. Read, G. W. Rubloff, L. L. Tedder, G. N. Parsons, *J. Vac. Sci. Technol.*, B15 (**1997**) 127-132.
[175] A. E. Kaloyeros, B. Zheng, I. Lou, J. Lau, J. W. Hellgeth, *Thin Solid Films*, 262 (**1995**) 20 -30.
[176] L. L. Tedder, G. W. Rubloff, I. Shareef, M. Anderle, D. - H. Kim, G. N. Parsons, *J. Vac. Sci. Technol.*, B13 (**1995**) 1924 - 1927.
[177] M. Juppo, A. Rahtu, M. Ritala, M. Leskelä, *Langmuir*, 16 (**2000**) 4034 - 4039.
[178] R. Matero, A. Rahtu, M. Ritala, M. Leskelä, T. Sajavaara, *Thin Solid Films*, 368 (**2000**) 1 -7.
[179] J. Hyvärinen, M. Sonninen, R. Törnqvist, *J. Gryst. Growth*, 86 (**1988**) 695 - 699.
[180] G. Sauerbrey, *Z. Phys.*, 155 (**1959**) 206 - 222.
[181] M. D. Ward, D. A. Buttry, *Science*, 249 (**1990**) 1000 - 1007.
[182] V. M. Mecea, J. O. Carlsson, P. Heszler, and M. Bârtan, *Vacuum*, 46(**1995**) 691 - 694.
[183] D. A. Buttry, M. D. Ward, *Chem. Rew.*, 92 (**1992**) 1355 - 1379.
[184] X. C. Zhou, L. Zhong, S. F. Y. Li, S. C. Ng, H. S. O. Chan, *Sensor. Actuat.*, B 42 (**1997**) 59 - 65.
[185] R. Lucklum, B. Henning, P. Hauptmann, K. D. Schierbaum, S. Vaihinger, W. Göpel, *Sensor. Actuat.*, A 25-27 (1991) 705-710.
[186] M. T. S. R. Gomes, M. O. Oliveira, J. A. B. P. Oliveira, *Langmuir*, 15 (**1999**) 8780-8782.
[187] M. Thompson, A. L. Kipling, W. C. Duncan-Hewitt, L. V. Rajakoviæ, B. A. Èaviæ-Vlasak, *Analyst*, 116 (**1991**) 881 - 890.
[188] E. P. Eernisse, *Applications of the Piezoelectric Quartz Crystal Microbalances*, (Eds: C. S. Lu, A. W. Czanderna), Elsevier, Amsterdam **1984**.
[189] V. E. Bottom, *Introduction to Quartz Crystal Unit Design*,Van Nostrand Reinhold, New York **1982**.
[190] J. Aarik, A. Aidla, A. Jaek, M. Leskelä, L. Niinistö, *J. Mater. Chem.*, 4 (**1994**) 1239-1244.
[191] E. B. Yousfi, J. Fouache, D. Lincot, *Appl. Surf. Sci.*, 153 (**2000**) 223 - 234.
[192] A. Rosental, A. Niilisk, *Surf. Sci.*, 307-309(**1994**)1188 - 1192.
[193] J. Aarik, A. Aidla, K. Kukli, *Appl. Surf. Sci.*, 75 (**1994**) 180-184.
[194] M. Ritala, M. Juppo, K. Kukli, A. Rahtu, M. Leskelä, *J. Phys. IV*, 9(**1999**) Pr8-1021 -1028.
[195] J.-F. Fan, K. Toyoda, *Appl. Surf. Sci.*, 60/61 (**1992**) 765-769.
[196] R. Matero, A. Rahtu, M. Ritala, *Chem. Mater.*, 13 (**2001**) 4506 - 4511.
[197] V. Sammelselg, A. Rosental, A. Tarre, L. Niinistö, K. Heiskanen, K. Ilmonen, L.-S. Johansson, T. Uustare, *Appl. Surf. Sci.*, 134 (**1998**) 78-86.

[198] J. Aarik, A. Aidla, A. - A. Kiisler, T. Uustare, V. Sammelselg, *Thin Solid Films*, 340 (**1999**) 110 - 116.
[199] K. Forsgren, A. Hårsta, J. Aarik, A. Aidla, *Electrochem. Soc. Proc.*, 2001-13 (**2001**) 152-159.
[200] J. C. Badot, S. Ribes, E. B. Yousfi, V. Vivier, J. P. Pereira-Ramos, N. Baffier, D. Lincot, *Electrochem. Solid-State Lett.*, 3 (**2000**) 485-488.
[201] J. Aarik, A. Aidla, K. Kukli, T. Uustare, *J. Cryst. Growth*, 144 (**1994**) 116-119.
[202] K., Kukli, J. Aarik, A., Aidla, O. Kohan, T. Uustare, V. Sammelselg, *Thin Solid Films*, 260 (**1995**) 135-42.
[203] H. Siimon, J. Aarik, *J. Phys. IV*, 5 (**1995**) C5-277 - 282.
[204] M. Pessa, R. Mäkelä, T. Suntola, *Appl. Phys. Lett.* 38 (**1981**) 131 - 132.
[205] K. Kukli, J. Aarik, A. Aidla, K. Forsgren, J. Sundqvist, A. Hårsta, T. Uustare, H. Mändar, A.-A. Kiisler, *Chem. Mater.* 13 (**2001**) 122-128.
[206] K. Knapas, A. Rahtu, M. Ritala, unpublished results.
[207] J.-F. Guillemoles, B. Canava, E. B. Yousfi, P. Cowache, A. Galtayries, T. Asikainen, M. Powalla, D. Hariskos, H.-W. Schock, D. Lincot, *Jpn. J. Appl. Phys.*, Part 1, 40 (**2001**) 6065-6068.
[208] F. Donsanti, B. Weinberger, P. Cowache, M. C. Bernard, D. Lincot, *Mat. Res. Soc. Symp. Proc.*, 668 (**2001**) H8.20/1- 8.
[209] E. B. Yousfi, B. Weinberger, F.Donsanti, P.Cowache, D. Lincot, *Thin Solid Films*, 387 (**2001**) 29-32.
[210] M. Juppo, A. Rahtu, M. Ritala, *Chem. Mater.*, 14 (**2002**) 281 - 287.
[211] B. V. Potapkin, private communications.
[212] L. Spassov, *Sensor. Actuat.*, A 30 (**1992**) 67 - 72.
[213] J. Ihanus, T. Hänninen, T. Hatanpää, T. Aaltonen, I. Mutikainen, T. Sajavaara, J. Keinonen, M. Ritala, M. Leskelä, *Chem. Mater.*, 14 (**2002**) 1937-1944.
[214] Y. Tsutsumi, M. Ikegawa, T. Usui, Y. Ichikawa, K. Watanabe, J. Kobayashi, *J.Vac. Sci. Technol.*, A14 (**1996**) 2337 - 2342.
[215] V.S. Ban, *J. Electrochem. Soc.*, 118 (**1971**) 1473 - 1477.
[216] M.Yoshida, H. Watanabe, F. Uesugi, *J. Electrochem. Soc.*, 132 (**1985**) 677 - 679.
[217] H. Toyoda, H. Kojima, H. Sugai, *Appl. Phys. Lett.*, 54 (**1989**) 1507 -1509.
[218] E. Clarke, *Thermochim. Acta*, 51 (**1981**) 7-15.
[219] M. R. Czerniak, B. C. Easton, *J. Crystal Growth*, 68 (**1984**) 128 - 135.
[220] C. M. McConica, D. A. Bell, K. L. Baker, D. Moss, *AIChE Journal* ,42 (**1996**) 1108 - 1115.
[221] Z. Liu, R. T. Lee, G. B.Stringfellow, *J. Cryst. Growth*, 191 (**1998**) 1 - 7.
[222] J.I. Davies, M. J. Parrott, J. O. Williams, *J. Cryst. Growth*, 79 (**1986**) 363 -370.
[223] W. L. Hsu, M. C. McMaster, M. E. Coltrin, D. S. Dandy, *Jpn. J. Appl. Phys.*, 33 (**1994**) 2231 - 2239.
[224] W. L. Hsu, D. M. Tung, *Rev. Sci. Instrum.*, 63 (**1992**) 4138 - 4148.
[225] A. Langer, J. T. Patton, *Vac. Microbalance Tech.*, 5 (**1966**) 231-245.
[226] D. C. Lay, *Linear Algebra and Its Applications*, Addison-Wesley Publishing Company, Reading MA, **1994**, p. 376.
[227] K. Kukli, M. Ritala, J. Sundqvist, J. Aarik, M. Leskelä, A. Hårsta, J. Lu, T. Sajavaara, Unpublished results.

[228] M. Putkonen, PhD Dissertation, Helsinki University of Technology, Inorganic Chemistry Publication Series, No.2, Espoo **2002**.
[229] M. Putkonen, L. Niinistö, *J. Mater. Chem.*, 11 (**2001**) 3141-3147.
[230] H.-J. Freund, *Faraday Discuss.*, 114 (**1999**) 1-31.
[231] M. Primet, P. Pichat, M. - V. Mathieu, *J. Phys. Chem.*, 75 (**1971**) 1216 - 1220.
[232] M. Zamora, A.Córdoba, *J. Phys. Chem.*, 82 (**1978**) 584 - 588.
[233] C. E. Nelson, J. W. Elam, M. A. Cameron, M. A. Tolbert, S. M. George, *Surf. Sci.*, 416(**1998**) 341 - 353.
[234] C. E. Nelson, J. W. Elam, M. A. Tolbert, S. M. George, *Appl. Surf. Sci.*, 171 (**2001**) 21-33.
[235] P. A. Agron, E. L. Fuller, H. F. Holmes, *J. Colloid Interf. Sci.*, 52 (**1975**) 553 -561.
[236] J. B. Peri, *Phys. Chem.*, 69 (**1965**) 211 - 219.
[237] S. M. George, A. W. Ott, J. W. Klaus, *J. Phys. Chem.*, 100 (**1996**)13121 - 13131.
[238] M. Ritala, T. Asikainen, M. Leskelä, *Electrochem. Solid-State Lett.*, 1(**1998**) 156 - 157.
[239] O.Ruff, J. Moczala, *Z. Anorg. Chem.*, 133 (**1924**) 193 - 219.
[240] G. B. Stringfellow, *Organometallic Vapor-Phase Epitaxy: Theory and Practice*, Academic Press inc. San Diego **1989**.
[241] M. Ritala, M. Leskelä, L. Niinistö, T. Prohaska, G. Friedbacher, M. Grasserbauer, *Thin Solid Films*, 250 (**1994**) 72-80.
[242] K.- E. Elers, M. Ritala, M. Leskelä, E. Rauhala, *Appl. Surf. Sci.*, 82-83 (**1994**) 468 - 474.
[243] P. Tägtström, P. Mårtensson, U. Jansson, J. O. Carlsson, *J. Electrochem. Soc.*, 146 (**1999**) 3139 - 3143.
[244] D. C. Bradley, R. C. Mehrotha, D. P. Gaur, *Metal Alkoxides*, Academic Press, London **1987**.
[245] G. A. M. Hussein, N. Sheppard, M. I. Zaki, R. B. Fahim, *J. Chem. Soc. Faraday Trans.* 87 (**1991**) 2661-2668.
[246] J. W. Elam, C. E. Nelson, M. A. Tolbert, S. M. George, *Surf. Sci.*, 450 (**2000**) 64-77.
[247] K. Kukli, M. Ritala, M. Leskelä, R. Lappalainen, *Chem. Vap. Deposition*, 4 (**1998**) 29 - 34.
[248] A. Vioux, *Chem. Mater.*, 9 (**1997**) 2292 - 2299.
[249] R. J. P. Corriu, D. Leclercq, P. Lefèvre, P. H. Mutin, A. Vioux, *J. Mater. Chem.*, 2 (**1992**) 673 - 674.
[250] J. Livage, C. Sanchez, *J. Non-Cryst. Solids*,145 (**1992**) 11 - 19.
[251] S. Chen, M. G. Mason, H. J. Gysling, G. R. Paz-Pujalt, T. N. Blanton, T. Castro, K. M. Chen, C. P. Fictorie, W. L. Gladfelter, A. Franciosi, P. I. Cohen, J. F. Evans, *J. Vac. Sci. Technol.*, A 11 (**1993**) 2419 - 2429.
[252] T. M. Mayer, J. W. Rogers, T. A. Michalske, *Chem. Mater*, 3 (**1991**) 641 - 646.
[253] A.C. Dillon, A. W. Ott, J. D. Way, S. M. George, *Surf. Sci.*, 322 (**1995**) 230 - 242.
[254] R. L. Puurunen, M.Lindblad, A. Root, A. O. I. Krause, *Phys. Chem. Chem. Phys.*, 3(**2001**)1093 - 1102.
[255] Joint Committee on Powder Diffraction Standards, Card 6-520, International Center for Diffraction Data, Newtown Square, PA.
[256] D. J. Burkey, T. P. Hanusa, *Acta Cryst.* , C52 (1996) 2452 - 2454.